Title

The Need for Near-Earth Multi-Spacecraft Heliospheric Measurements and an Explorer Mission to Investigate Interplanetary Structures and Transients in the Near-Earth Heliosphere.

Journal

Space Science Reviews, 220(7)

ISSN

0038-6308

Authors

Lugaz, Noé

Lee, Christina

Al-Haddad, Nada

et al.

Publication Date

2024

DOI

10.1007/s11214-024-01108-8

Peer reviewed

Space Science Reviews (2024) 220:73
https://doi.org/10.1007/s11214-024-01108-8

SPECIAL COMMUNICATION

The Need for Near-Earth Multi-Spacecraft Heliospheric Measurements and an Explorer Mission to Investigate Interplanetary Structures and Transients in the Near-Earth Heliosphere

Noé Lugaz[1] · Christina O. Lee[2] · Nada Al-Haddad[1] · Robert J. Lillis[2] · Lan K. Jian[3] · David W. Curtis[2] · Antoinette B. Galvin[1] · Phyllis L. Whittlesey[2] · Ali Rahmati[2] · Eftyhia Zesta[3] · Mark Moldwin[4] · Errol J. Summerlin[3] · Davin E. Larson[2] · Sasha Courtade[2] · Richard French[5] · Richard Hunter[5] · Federico Covitti[5] · Daniel Cosgrove[2] · J.D. Prall[5] · Robert C. Allen[6] · Bin Zhuang[1] · Réka M. Winslow[1] · Camilla Scolini[1,7] · Benjamin J. Lynch[2,8] · Rachael J. Filwett[9] · Erika Palmerio[10] · Charles J. Farrugia[1] · Charles W. Smith[1] · Christian Möstl[11] · Eva Weiler[11] · Miho Janvier[12] · Florian Regnault[1] · Roberto Livi[2] · Teresa Nieves-Chinchilla[3]

Received: 6 February 2024 / Accepted: 9 September 2024 / Published online: 20 September 2024

Abstract
Based on decades of single-spacecraft measurements near 1 au as well as data from heliospheric and planetary missions, multi-spacecraft simultaneous measurements in the inner heliosphere on separations of 0.05–0.2 au are required to close existing gaps in our knowledge of solar wind structures, transients, and energetic particles, especially coronal mass ejections (CMEs), stream interaction regions (SIRs), high speed solar wind streams (HSS), and energetic storm particle (ESP) events. The Mission to Investigate Interplanetary Structures and Transients (MIIST) is a concept for a small multi-spacecraft mission to explore the near-Earth heliosphere on these critical scales. It is designed to advance two goals: (a) to determine the spatiotemporal variations and the variability of solar wind structures, transients, and energetic particle fluxes in near-Earth interplanetary (IP) space, and (b) to advance our fundamental knowledge necessary to improve space weather forecasting from *in situ* data. We present the scientific rationale for this proposed mission, the science requirements, payload, implementation, and concept of mission operation that address a key gap in our knowledge of IP structures and transients within the cost, launch, and schedule limitations of the NASA Heliophysics Small Explorers program.

Keywords Coronal mass ejection · Interplanetary space · Mission concept

Note by the Editor: This is a Special Communication. In addition to invited review papers and topical collections, Space Science Reviews publishes unsolicited Special Communications. These are papers linked to an earlier topical volume/collection, report-type papers, or timely papers dealing with a strong space-science-technology combination (such papers summarize the science and technology of an instrument or mission in one paper).

Extended author information available on the last page of the article

1 Introduction

High-speed solar wind streams (HSS), stream interaction regions (SIRs), and interplanetary (IP) transients, such as coronal mass ejections (CMEs) and IP shocks, are large-scale structures that are the main drivers of space weather effects in near-Earth space and the main accelerators of energetic particles in the inner heliosphere. They constitute a unique plasma environment, where many fundamental plasma processes (magnetic reconnection, particle acceleration, etc.) can be tested in an environment that differs significantly from the typical solar wind (e.g., low beta plasma in CME ejecta, hot and dense plasma in SIRs and CME sheaths). By nature, these transients and structures vary temporally and spatially as they are measured by spacecraft (e.g., see Winslow et al. 2021; Lugaz et al. 2022; Regnault et al. 2023). Our understanding of the properties of these streams, structures, and transients has been built primarily on single-point *in situ* measurements obtained from 0.1 au (Parker Solar Probe, see Fox et al. 2016; Raouafi et al. 2023) to several tens of au (Pioneer, Voyager, and New Horizons) with most measurements to date having occurred between 0.3 au (Helios, MESSENGER, Solar Orbiter) and 5.4 au (Ulysses, Juno), including near 1 au by missions such as IMP-8, ISEE-3, Wind, ACE, and STEREO. However, large-scale structures are rarely measured simultaneously by more than one spacecraft on spatial scales large enough to enable investigations of the variations of their properties (such as their shape, size, extent, orientation) in space and time. As detailed below, multi-spacecraft measurements at proper separations are required to investigate the spatiotemporal variations within solar wind streams, SIRs, CMEs (including their sheath regions and magnetic ejecta), IP shocks, and locally-accelerated energetic particles, as well as the variability from one event to another.

A few multi-spacecraft measurements have highlighted both the limitations of the approach to date to explore the nature of CMEs as well as the variability of solar wind streams and energetic particles (see e.g. Neugebauer et al. 2006; Ebert et al. 2016; Lugaz et al. 2018, 2022, 2024; Ala-Lahti et al. 2020; Winslow et al. 2021; Kouloumvakos et al. 2022). For example, when the twin STEREO spacecraft orbited through the near-Earth heliosphere for six months in 2007, they revealed that dramatic differences in the properties of these large-scale structures can appear on separations of 1–20° of heliospheric longitude (Kilpua et al. 2011). Additional similar multi-spacecraft measurements are needed to investigate and determine the effects of shock and turbulence properties on the local acceleration of particles and the three-dimensional (3D) configuration and time-dependent nature of solar wind streams and transients.

In addition, one of the main space weather threats is associated with the arrival of IP shocks at Earth, with potential catastrophic consequences from the associated geomagnetically induced currents (GICs, see for example Oliveira et al. 2018). Currently, IP shock properties and accurate arrival times can only be reliably forecasted from *in situ* measurements, and current 15-to-60-minute lead times provided by L1 measurements are often not sufficient for mitigation. While remote observations can provide arrival time forecasts and estimates of the shock speed, arrival times based on remote-sensing observations have mean absolute errors of about 10 hours (e.g., see Riley et al. 2018; Kay et al. 2024) and mean absolute speed errors of 100 km s^{-1}. Shocks, CMEs, and solar wind streams have never been reliably and consistently measured upstream of L1 to forecast their consequences on space assets and the power grid with lead times on the order of several hours, although Solar Orbiter has provided some recent proof-of-concept for such measurements (Laker et al. 2024). Sub-L1 or Solar Sentinels have been proposed for more than two decades to improve upon this timing (St. Cyr et al. 2000). However, before launching such operational space weather missions, in-depth scientific investigations are required to understand how the solar wind

and associated transients evolve during their propagation from the spacecraft to Earth (or L1) and to determine the optimal mission configuration.

Breakthroughs in our understanding of geospace have been made through measurements from multi-spacecraft missions in the magnetosphere –the Time History of Events and Macroscale Interactions during Substorms (THEMIS, Angelopoulos 2008) and Cluster (Escoubet et al. 1997)– and across the bow shock and magnetotail (the Magnetosphere MultiScale [MMS] mission, Burch et al. 2016). Multi-spacecraft missions are under development to provide multi-point measurements of plasma turbulence (HelioSwarm, see Klein et al. 2023) and of magnetosphere–ionosphere coupling (Geospace Dynamics Constellation [GDC], Pfaff 2016). No existing or past mission has provided dedicated *in situ* measurements of the inner heliosphere with three or more spacecraft. This clearly hinders our progress in understanding the interplanetary magnetic field (IMF) and the solar wind, its structures and transients, and particle acceleration and in moving towards more advanced space weather forecasting platforms and techniques. In addition, the near-Earth heliosphere, which we define here as the region ranging from about 0.01 au to 0.25 au from Earth was only briefly traveled through by STEREO and *Wind*. We chose 0.25 au as it corresponds approximately to the heliocentric distance between Earth and Venus at inferior conjunction and 0.01 au as it corresponds to the heliocentric distance between the Sun–Earth L1 point and Earth. Both STEREO A and B spacecraft spent seven months within 10° ($\sim$0.25 au) of the Sun–Earth line during a deep solar minimum in 2007 and STEREO-A just traversed this region over ten months from 2023 May to 2024 March. *Wind*'s extended mission included two distant prograde orbits (Franz 2002; Wilson et al. 2021) that ventured 0.7° from the Sun–Earth line in 2000–2002.

Multi-spacecraft missions in the inner heliosphere with *in situ* instrumentation dedicated to large-scale structures have been proposed for several decades. The 2003 United States Heliophysics Decadal Survey (National Research Council 2003) ranked a MultiSpacecraft Heliospheric Mission (MHM) as Medium-scale priority number 4. The MHM concept consisted of "four or more spacecraft with large separations in the ecliptic plane to determine the spatial structure and temporal evolution of CMEs and other solar-wind disturbances in the inner heliosphere." It also ranked a Solar Wind Sentinels mission ("Three spacecraft [...] to provide earlier warning than L1 monitors and to measure the spatial and temporal structure of CMEs, shocks, and solar-wind streams") as Medium-scale priority number 8. All mission concepts with higher priority than MHM have been at least partially implemented: Parker Solar Probe as the only large-scale mission, MMS, the Van Allen Probes (Mauk et al. 2013), and Juno for the top three medium-scale missions. In the recent NASA Space Weather Gap Analysis (see Vourlidas et al. 2023), solar wind observations, including off the Sun–Earth line, were ranked as one of the top priorities to fill the critical observational gaps (see Fig. 1). The Space Weather Diamond mission concept of St. Cyr et al. (2000), as well as the HELIospheric eXplorers (HELIX, Szabo et al. 2023) mission, are some concepts that have been proposed to address some of these limitations.

Here, we discuss the rationale, requirements and a summary of the implementation for the Mission to Investigate Interplanetary Structures and Transients (MIIST), a streamlined Class-D mission that was proposed to NASA Heliophysics division as a Small Explorer (SMEX) in 2022. MIIST has two goals: (a) to determine the spatiotemporal variations of solar wind structures, transients, and energetic particles in near-Earth IP space, and (b) to advance the fundamental knowledge necessary to improve space weather forecasting from *in situ* data. In the rest of this article, we first describe in Sect. 2 the science rationale, the science questions to be addressed and the measurement requirements for the mission. In Sect. 3, we briefly describe the overall implementation to reach those requirements, namely

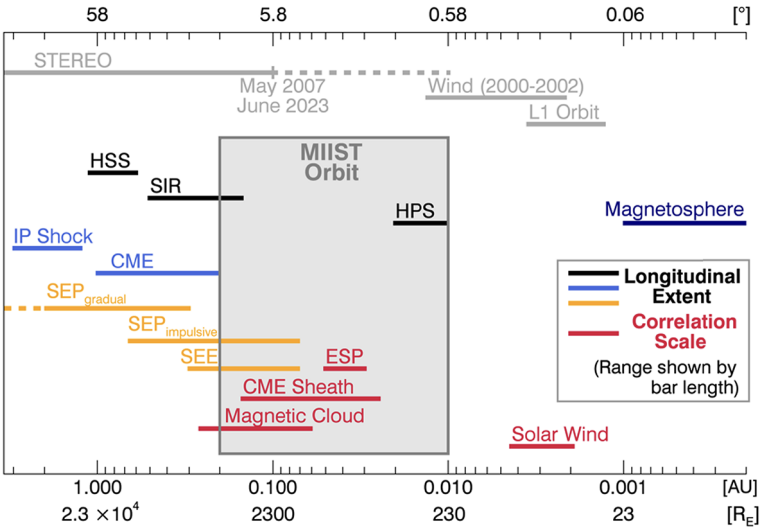

Fig. 1 Overview of the key scales of near-Earth interplanetary structures (black bars), transients (blue bars) and energetic particles (orange bars) and the correlation lengths (crimson bars) of energetic storm particle (ESP) events, CME sheaths and ejecta and the size of solar energetic electron (SEE) events. These summarize several dozens studies over the past two decades, as discussed in the text. The MIIST orbit (grey box) is optimized to ensure that most structures, transients, and energetic particles impacting Earth are measured by four identical spacecraft. The various L1 orbits, *Wind* prograde orbit of 2000–2002 and STEREO near-Earth passes in 2007 and 2023–2024 are shown in grey colors

the instrument payload, orbit, and number of spacecraft. In Sect. 4, we describe the spacecraft design, concept of operations and propulsive maneuvers. We conclude in Sect. 5.

2 Science Rationale, Science Objectives and Measurement Requirements

We first summarize the existing knowledge gaps and science justification for a multi-spacecraft near-Earth heliospheric mission, which are organized over the main themes of solar wind streams, CMEs and IP shocks, energetic particles, and space weather. Each section starts with an introduction to the science topic, lists past multi-spacecraft measurements and explains why there is a gap in our understanding of these phenomena that requires dedicated simultaneous multi-spacecraft measurements. Then, we present how these knowledge gaps correspond to specific science and research objectives and provide the observation requirements in order to achieve them.

2.1 Knowledge Gap 1: Longitudinal and Temporal Variations in the Properties of IP Structures

Solar Wind Streams, Stream Interaction Regions, Heliospheric Current and Plasma Sheets SIRs form when a fast solar wind streams catches up with a slow solar wind stream (e.g., see Richardson 2018). They are the main source of moderate geomagnetic storms, and second to CMEs in terms of driving intense space weather (Tsurutani et al. 2006; Zhang et al. 2007; Echer et al. 2013). HSS and SIRs can have severe effects on Earth's radiation belts and

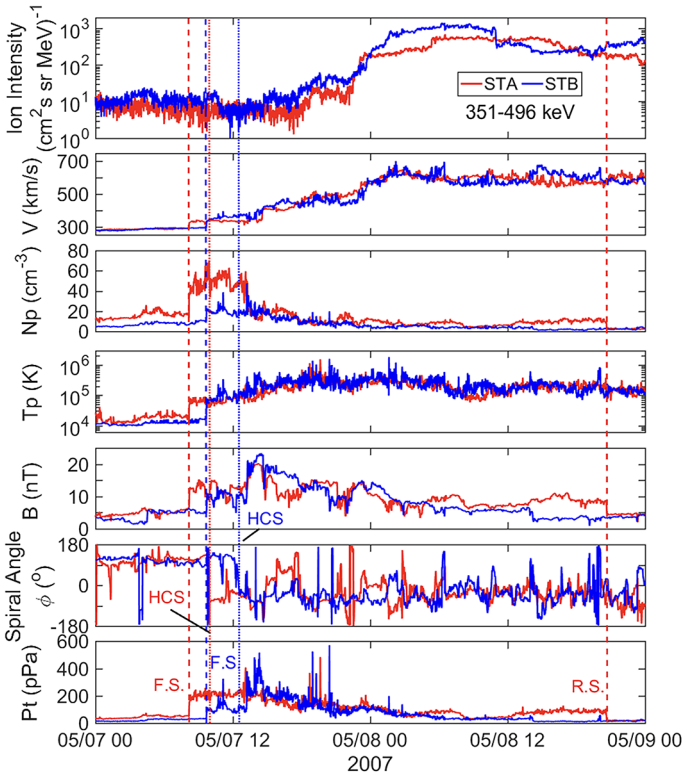

Fig. 2 SIR on 2007 May 7–8 when the longitudinal separation between STEREO-A (red lines) and STEREO-B (blue lines) was 7°. Adapted from Jian et al. (2009). Forward shocks (F.S.) are marked by dashed lines. A reverse shock (R.S.) at STEREO-A is marked by a dashed line. The HCS is marked by a dotted line. The panels show from top to bottom the suprathermal ion flux around 400 keV, the proton velocity, density, temperature, the magnitude of the magnetic field, the east-west magnetic field angle and the total pressure (sum of the magnetic and thermal pressures)

plasma sheet (e.g., see Denton and Borovsky 2008; Miyoshi et al. 2013; Souza et al. 2017), even during moderate storms. About 20–30% of SIRs drive shocks at 1 au (Jian et al. 2006, 2019) and about 3% of them drive shocks at 0.72 au (Jian et al. 2008a), suggesting the near-Earth heliosphere, especially upstream of L1 is likely an incubator of SIR-driven shocks. These shocks are able to accelerate ions to energies in the range from tens of keV to a few MeV (e.g., Cohen et al. 2020).

Heliospheric current sheet (HCS) crossings can be detected by a reversal in the magnetic field direction, as can also be inferred from the reversal of the direction of the strahl of suprathermal electrons (e.g., see Smith 2001). An example of a HCS crossing is shown in Fig. 2. The heliospheric plasma sheet (HPS) surrounds the HCS and is characterized by an enhanced proton number density and plasma β (Winterhalter et al. 1994; Crooker et al. 2004) and a decreased magnetic field. The HPS and HCS often have embedded CMEs or small transients (Moldwin et al. 2000; Yu et al. 2014). The interaction of CMEs with HCSs and HPSs, and their propagation within these regions, is dynamic and often renders the interpretation of single-spacecraft *in situ* measurements of CMEs or HPS highly ambiguous (Winslow et al. 2016).

Past Multi-Spacecraft Measurements and Their Limitations Most dedicated multi-spacecraft measurements of solar wind streams and structures have been made with the twin STEREO spacecraft, sometimes combined with L1 missions. Between 2007 and 2014 (loss of STEREO-B), STEREO-A and STEREO-B were apart, on average, by 0.1 au in heliocentric distance and 1–6° latitudinally, with their longitudinal separation varying between 0 and 180°. With two-spacecraft measurements, it is impossible to distinguish the effects associated with radial, longitudinal, and latitudinal variations. For example, the May 2007 SIR (Fig. 2) was measured at 0.96 au by STEREO-A with a developing pair of forward–reverse shocks, but only with a forward shock at 1.05 au by STEREO-B. This example demonstrates that measurements from two spacecraft alone cannot clearly distinguish if the differences in the observations were due to the radial (∼0.09 au) and longitudinal (∼7°) separations between the spacecraft, and/or due to the intrinsic tilt of the SIR.

Need for Simultaneous Multi-Spacecraft Measurements To advance our understanding of solar wind streams and structures, simultaneous multi-point measurements of the plasma and IMF parameters are needed for the majority of solar wind streams and structures reaching L1 with spacecraft separated longitudinally, radially, and along the Parker spiral. Studying spatiotemporal variations in the solar wind streams and structures requires at least three spacecraft, with a fourth SC necessary to investigate the influence of latitudinal effects (such as the tilt of SIRs, HCSs, etc.). To study the temporal evolution of solar wind structures, the separation between the spacecraft should be in the range of 0.5° to 20° to capture the scales of HPS and SIRs (see Fig. 1). However, simultaneous multi-point measurements of SIRs over at least 25% of their typical longitudinal extent (i.e. longitudinal separations $> 6°$) are needed to investigate how SIR evolve as they pass over 1 au. Figure 2 shows the clear difference in the stream interface, especially the density for a SIR measured by two spacecraft at 7° of longitudinal separations. Future measurements should ensure that at maximum longitudinal separations, the heliocentric distances of the spacecraft are nearly identical, contrary to the case presented in this picture, so that propagation effects are minimal.

2.2 Knowledge Gap 2: Global Configuration of Interplanetary Transients

Coronal Mass Ejections and IP Shocks CMEs are at the center of solar-terrestrial physics: they are the main cause (∼80%) of intense geomagnetic storms (Zhang et al. 2007; Echer et al. 2008; Kilpua et al. 2017) and are essential to understanding the global heliospheric flux budget (Owens and Crooker 2006; Smith et al. 2014; Winslow et al. 2023). A CME is a large propagating structure of magnetically dominated plasma (the magnetic ejecta or ME) that drives a dense sheath, often preceded by a fast-forward shock (Manchester et al. 2017). Because magnetic fields cannot be reliably measured remotely in the corona and IP space, nearly all of what we know about the magnetic structure of the ejecta comes from *in situ* measurements.

Fast IP shocks are the main locus of particle acceleration (Lee et al. 2012; Reames 2013), while CME sheath regions, made of solar wind compressed by the shock, are one type of major drivers of geomagnetic activity (Huttunen and Koskinen 2004; Echer et al. 2013; Oliveira and Raeder 2015; Lugaz et al. 2016). Shock characteristics can be determined using the Rankine–Hugoniot relations (Vinas and Scudder 1986; Koval and Szabo 2008).

Past Multi-Spacecraft Measurements and Their Limitations The large majority (>90%) of CMEs are only measured at one point in space (see Fig. 3), which limits the accuracy of reconstruction models (Al-Haddad et al. 2013). Magnetic clouds (MCs) with their well-defined properties (Burlaga et al. 1981) are often thought as the quintessential magnetic

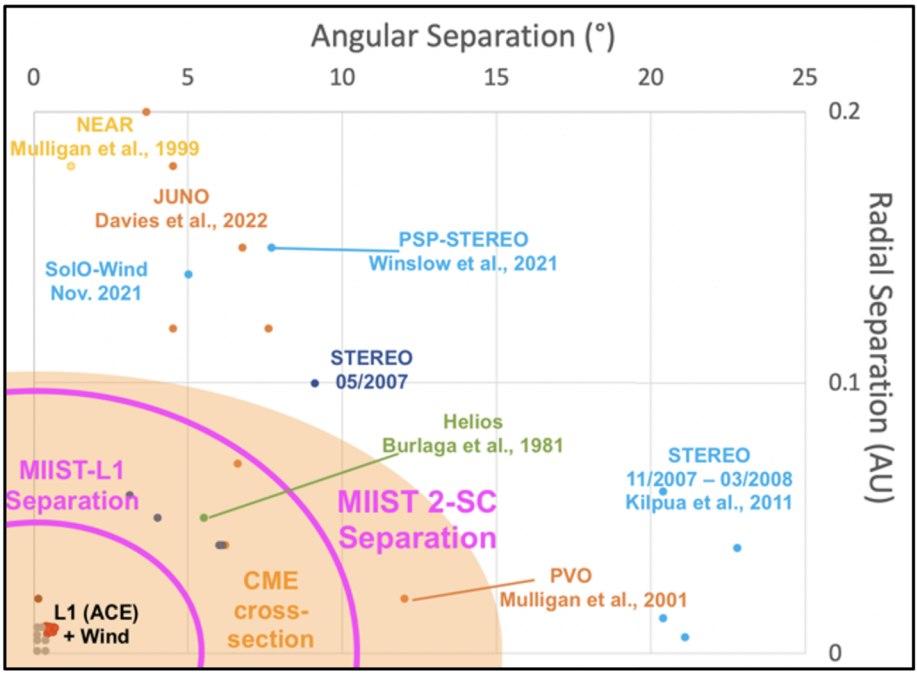

Fig. 3 Past multi-spacecraft measurements of CMEs up to early 2021 (adapted from Lugaz et al. 2018 with updates), typical shape of the cross section of a MC following Démoulin et al. (2016), and the 2-spacecraft separations made possible by MIIST. Many such past multi-spacecraft measurements partially rely on planetary missions which often only include magnetic field (no plasma) measurements. STEREO-A in 2022–2023 enabled 10–20 additional 2-spacecraft measurements within the critical region of 0–0.1 au of radial separation and 0–15° of angular separation, which are currently under analysis

configuration of CMEs, and yet, only one third of CMEs measured near 1 au are identified as MCs. It remains unclear if all CMEs are MCs with some of them not measured as such due to the CME trajectory with respect to the spacecraft, or if there are multiple magnetic configurations inside CMEs (Lynch et al. 2010; Al-Haddad et al. 2019). Lugaz et al. (2018) highlighted notable differences in the CME global magnetic field measured simultaneously by ACE and *Wind* for separations of 0.5–0.7°, whereas the investigation of the May 2007 CME (Liu et al. 2008; Möstl et al. 2009; Mulligan et al. 2013) highlights how two spacecraft separated by 9° may not measure the same event at all. These surprising results emphasize how little is known about the global magnetic configuration of CMEs. Regnault et al. (2023) recently used simultaneous measurements with two spacecraft radially aligned and separated by 0.05–0.2 au to showcase how CME magnetic fields change significantly during the duration of a spacecraft crossing (as the CME ages by ∼1 day throughout the crossing). These changes have not been investigated in a comprehensive manner due to the lack of adequate measurements. Assumptions, such as force-free (Lepping et al. 1990), self-similar, or static nature of CMEs, have been utilized out of neccesity to develop models of CMEs based on single-spacecraft measurements. At least three sets of simultaneous and independent measurements, with radial and longitudinal separations, are necessary to test these physical assumptions. A fourth set of measurements is required to further investigate CME extent and orientation.

Multi-spacecraft measurements near L1 by *Wind*, ACE, DSCOVR, and SOHO can be used to better constrain their derived properties (e.g., see Koval and Szabo 2010; Stevens et al. 2018), but they only provide local information about the shocks. From observations and simulations, the acceleration of particles by shocks is known to depend fundamentally on the shock normal angle, θ_{Bn}, the angle between the upstream magnetic field and the shock normal, with different physical mechanisms occurring for quasi-parallel ($\theta_{Bn} \sim 0°$) and quasi-perpendicular ($\theta_{Bn} \sim 90°$) shocks. However, little is known from observations about the way θ_{Bn} varies along the shock front on intermediate scales of 1–20°, i.e., about the global radius of curvature of the shock. For CME-driven shocks, the radius of curvature is thought to be 0.2–1 AU (e.g., see Koval and Szabo 2010).

Need for Simultaneous Multi-Spacecraft Measurements To advance our understanding of solar wind transients, simultaneous multi-point measurements of the plasma and IMF parameters are needed for the majority of CMEs and shocks reaching L1 with spacecraft separated longitudinally and radially. Figure 3 highlights that longitudinal separations of 5–10° are ideal to investigate CMEs, which is also confirmed by a recent study (Lugaz et al. 2024) of MEs measured simultaneously by STEREO-A and spacecraft at L1 in 2022. As highlighted in recent work (Regnault et al. 2023, 2024a,b), separations in heliocentric distances of 0.1–0.2 au are ideal to investigate the aging of CMEs as they reach 1 au and to determine their true, time-independent properties.

2.3 Knowledge Gap 3: Dependence of Particle Acceleration by IP Structures and Transients on Local and Global Conditions

Energetic Storm Particles and SIR-Accelerated Particles Energetic storm particles (ESPs) are particles locally accelerated by an IP shock and have typical energies between ~100 keV and ~5 MeV. They occur on average for only 15–35% of the shocks (Lario et al. 2003; Giacalone and Jokipii 2012) measured near 1 au. ESP events are typically classified according to their temporal profile shapes as spike, rise, step, flat, and complex types. There is no simple relationship between the presence/absence of ESP events, their type, and characteristics of the shock such as speed, Mach number, or shock normal angle (Neugebauer and Giacalone 2005; Neugebauer et al. 2006). In particular, the way the acceleration of particles at various locations along the shock front differs based on the global and local conditions is still poorly understood.

SIR-associated energetic particles are typically of the same energies as ESPs (100 keV–5 MeV). Near solar minimum, they represent the primary source of energetic particles in the heliosphere. Shocks (forward and reverse) associated with SIRs are thought to be the loci where these particles are accelerated. As most SIRs form shocks between 0.7 and 5 au (Jian et al. 2006, 2008a,b), many of these particles measured near 1 au propagate sunward from the shock acceleration location, which is beyond 1 au. In addition, compression regions that form earlier than shocks play a role in accelerating particles, but often to lower energies (Giacalone et al. 2002).

Past Multi-Spacecraft Measurements and Their Limitations Understanding how the particle properties depend on local and global properties requires multi-spacecraft measurements of ESP events. Ebert et al. (2016) performed such a study for shocks measured for longitudinal separations of 60–120° and concluded that different upstream conditions, including turbulence and seed particles, strongly affect the ESP characteristics. No such study has been performed for intermediate separations for which the properties of the shocks accelerated

the ESPs could still be well correlated from one spacecraft to the next. The analyses of 86 ESP events measured by ACE and *Wind* for small longitudinal separations (0.7°) revealed that the ESP measurements become less correlated as the spacecraft separation increases (Neugebauer and Giacalone 2005; Neugebauer et al. 2006). These studies suggest that the profile shape of ESP events measured by two spacecraft at longitudinal separations of 2.5° will always be different, but this needs to be tested.

Studies (Gómez-Herrero et al. 2009; Bučík et al. 2011) investigated solar energetic particle (SEP) events related to SIRs during the early phase of the STEREO mission and showed large variations in fluxes (factor of 2–10), even for small angular separations (e.g., see the top panel of Fig. 2). However, the flux variations due to separations in radial distance, latitude, and longitude are compounded for STEREO measurements.

Need for Simultaneous Multi-Spacecraft Measurements Simultaneous multi-point measurements of the IP structures that accelerate particles and those energetic particle must be made (a) for spacecraft separated by ∼0.1 au along the Parker spiral from each other to provide measurements of energetic particles along a field line magnetically connected to two spacecraft with separations that result in differences in particle arrival time (about 15–20 minutes for a 1 MeV proton), and (b) separations of at least 2–5° from each other (based on past studies of ESPs), while at nearly the same heliocentric distance, to provide multi-spacecraft measurements of shocks and energetic particles along a shock front.

2.4 Knowledge Gap 4: Space Weather Research with Upstream Solar Wind Monitors

Forecasting the Arrival and Properties of Potential Geo-Effective Structures and Transients from in-Situ Measurements For corotating structures, forecasting their arrival and properties ahead of time either can be done (i) from remote observations of coronal holes (e.g., see Hofmeister et al. 2022; Kay et al. 2023), (ii) using empirical or physics-based models that link the solar wind properties to the solar magnetic field as measured by magnetograms (e.g., see Arge and Pizzo 2000; Cohen et al. 2007; van der Holst et al. 2014), or (iii) from *in situ* measurements. For *in situ* measurements, it requires an assumption of persistence (a structure measured at L1 will be measured identically one Carrington rotation later) or the use of STEREO measurements, for which the longitudinal separation between the Sun–Earth line and the Sun–spacecraft line has varied from 0° to ±180° throughout the mission.

Since mid-2023, with STEREO-A on the west side of the Sun–Earth line and STEREO-B no longer operational, such measurements are not available. Other methods using solar or heliospheric remote-sensing observations can provide forecast of some (for example, the peak velocity) but not all properties of IP structures, especially the north–south component of the magnetic field, B_z.

For radially propagating transients, L1 provides a 15-to-60-min warning of upcoming transients (for speeds of 400–1600 km s^{-1}) before they impact the magnetosphere. Sub-L1 monitors have been proposed for more than two decades (St. Cyr et al. 2000; West 2005; Akhavan-Tafti et al. 2023) to improve upon this timing. However, space weather research is first required to determine how best to forecast the properties and geo-effectiveness of radially propagating transients from such monitors.

Past Studies and Their Limitations For corotating structures, past work has shown that using STEREO measurements leads to an improved forecast as compared to assuming persistence, but the improvement decreases significantly both with increasing longitudinal separations and with latitudinal separation (Thomas et al. 2018; Bailey et al. 2020; Allen et al. 2021;

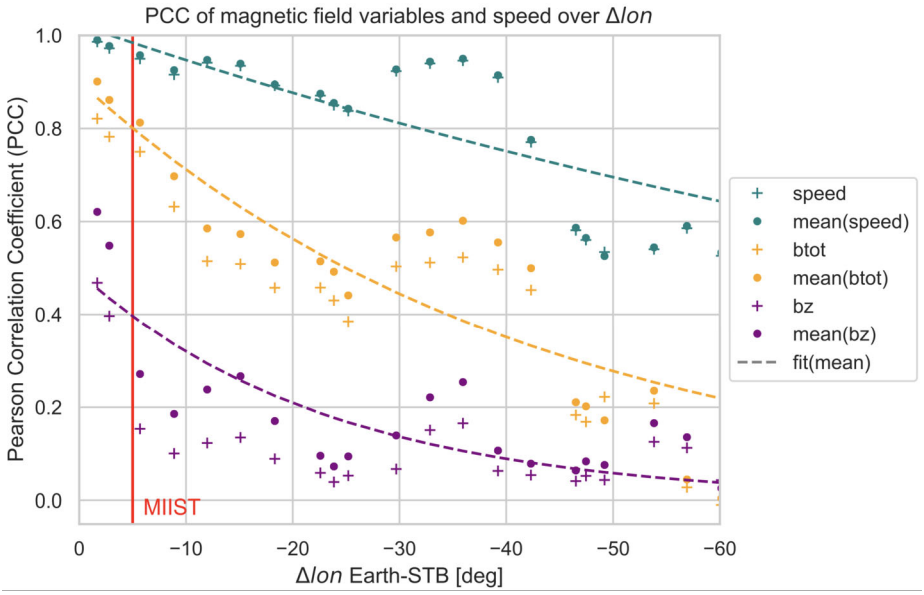

Fig. 4 Correlation of the IMF and solar wind speed between STEREO-B and L1 as a function of the longitudinal separation in 2006–2008. The solar wind speed measured at two spacecraft separated by <60° is well correlated (Pearson correlation, PCC > 0.5), the same does not hold true for the IMF magnitude beyond 20° or for B_z beyond ∼5°. Adapted from Bailey et al. (2020)

Chi et al. 2022). With an L5 space weather mission such as Vigil, which is currently planned by ESA (Palomba and Luntama 2022), only the speeds of corotating structures would be well correlated between L1 and L5 (at 60° separation, see Fig. 4). Further work is needed to investigate the optimal distance from Earth to forecast corotating structures.

For radially propagating transients, past studies (Lindsay et al. 1999; Kubicka et al. 2016; Möstl et al. 2018) have used Pioneer Venus Orbiter, Venus Express, or MESSENGER data to study the appropriateness of far-upstream measurements to predict Kp and Dst at Earth, but no such study has been done for measurements within 0.01–0.1 au from L1, due to the lack of adequate measurements.

Additional studies are made possible by the recent passage of STEREO-A upstream of Earth in mid-2023, the data for this time period is still being analyzed. Figure 5 shows an interval of CME and SIR observations with STEREO-A and *Wind* in April and May 2023, when STEREO-A approached the Sun–Earth L1 point and was sunward of L1 by about 0.05 au. It passed in front of L1 in August 2023. These data are still to be analyzed, but recent proof-of-concept studies for CMEs have been performed with Solar Orbiter (Davies et al. 2021; Laker et al. 2024) for events in April 2020 and March 2022, with Solar Orbiter at heliocentric distances of ∼0.81 and ∼0.46 au, respectively. Meanwhile, recent work by Regnault et al. (2024a) showed that there can be some significant differences between CME measurements for two spacecraft within less than 2° of angular separation and ∼0.15 au of radial separation. Furthermore, Palmerio et al. (2024) investigated the structure of a CME encountered in February 2022 by BepiColombo and Parker Solar Probe at ∼0.35 au, the two probes being characterized by an angular separation of 5° and a radial separation of 0.03 au, and found drastic differences between the two sets of measurements—highlighting

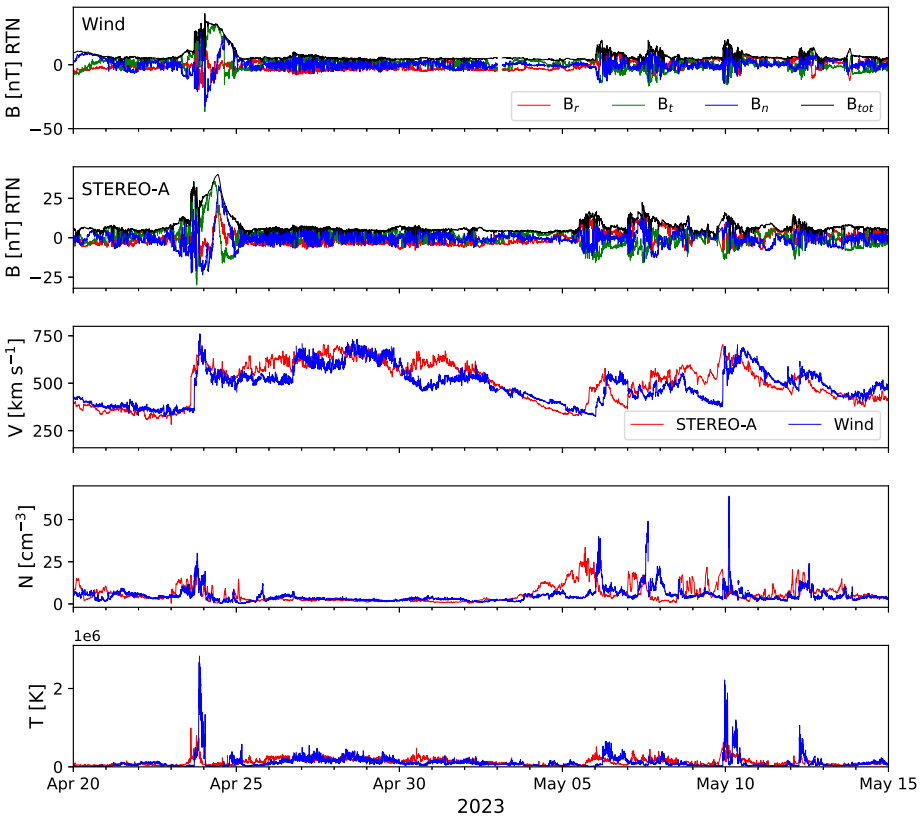

Fig. 5 *In situ* measurements of solar wind plasma and magnetic field parameters by STEREO-A and *Wind* in April and May 2023. Several CMEs and CIRs have impacted both spacecraft, while STEREO-A was positioned 0.05 au closer to the Sun, moving from −10.4° to −8.5° longitude (HEEQ) during the plot interval. For corotating structures, this should correspond to STEREO-A measuring streams ∼12–18 hours earlier than *Wind*

that variations in CME internal structure can be prominent even at Mercury's orbit, where CMEs are expected to have experienced less evolutionary changes than at 1 au.

Need for Additional Measurements IP structures can experience significant evolutionary changes in the last 12–24 hours before impacting L1, which can result in significant errors in forecasting. It is unclear how close to the Sun–Earth line measurements must be taken to be useful for space weather forecasting. Many transients have a small (∼5°) non-radial propagation direction. There can also be significant non-radial flows associated with IP shocks and CME sheaths (Al-Haddad et al. 2022). On the one hand, a sub-L1 monitor on the Sun–Earth line, as made possible by solar sail technology, might not be the most appropriate forecasting platform if such non-radial flows are common. On the other hand, measurements obtained at more than 5–10° from the Sun–Earth line may not reflect the conditions that are experienced at Earth based on the few aforementioned studies of differences in CME properties between two spacecraft at separations of 5–10°. For example, Fig. 5 shows similarities in the magnetic field profile (specifically the components) of the CME on 2023 April 23–24 but also differences in the overall shape of the magnetic field strength

profile as well as some differences in the measured velocity. To increase the lead times of most solar wind transients from 40–60 minutes to 2.5–4 hours, measurements should occur from at least 0.03 au sunward of L1. To investigate the forecasting of corotating streams and the influence of moderate separations from the Sun-Earth line, measurements should be taken at various separations from the Sun-Earth line with maximum longitudinal separation reaching at least 5° east of the Su-Earth line, separations at which the correlation between L1 and a spacecraft measurements for B_z reach 0.5 (see Fig. 4).

2.5 Mission Science Objectives

Based on these identified gaps and need for multi-spacecraft measurements, specific science objectives (SOs) and space weather research objectives (SWROs) can be identified:

(SO1) Characterize how solar wind streams and SIRs vary in the inner heliosphere.

(SO2) Determine the global configuration of CMEs and IP shocks near 1 au.

(SO3) Quantify how particle acceleration at shocks and compression regions depend on local and global conditions and vary depending on longitude.

(SWRO1) Provide real-time beacon data of the solar wind, energetic particles, and transients upstream of L1.

(SWRO2) Provide real-time beacon data of the solar wind, east of the Sun–Earth line.

(SWRO3) Determine how far away from the Sun–Earth line and how far sunward of L1 future space weather monitors should be placed for optimum forecasting.

(SWRO4) Investigate how measurements sunward of L1 can be best used to forecast geomagnetic activity.

2.6 Measurement Requirements

To close the knowledge gaps and meet the SOs and SWROs, a mission must measure the plasma and magnetic field of CMEs, IP shocks, and SIRs for the vast majority of expected conditions near 1 au. Thanks to several decades of consistent measurements from near 1 au by IMP-8, ISEE-3, *Wind*, ACE and STEREO, the measurement requirements in term of solar wind plasma and IMF are well known (e.g., see Jian et al. 2018, 2019; Nieves-Chinchilla et al. 2018, for database of SIRs and CMEs over the past decades). CMEs and SIRs are the leading causes of extreme values of magnetic field, density (both low and high for CMEs), velocity, non-radial flows, temperature, and dynamic pressure. For example, the highest solar wind speed ever measured near 1 au is about 2300 km s^{-1} for the 2012 July 23 CME measured by STEREO-A (Liu et al. 2014), which was associated with an IMF magnitude of ∼110 nT.

Based on OMNI data over the past 30 years, 99.9% of the 1-hour average of the measured proton velocity were below 820 km s^{-1}, 99.9% of the 1-hour average of the proton density were below 46 cm^{-3}, and 99.9% of the 1-hour dynamic pressure were below 18 nPa, while 99.9% of the 1-hour IMF magnitude were below 28 nT. 1-min measurements do reach higher extremes than those listed here. Focusing on the four years in the interval 2000–2003 during the maximum of Solar Cycle 23, the proton velocity reached up to 1000 km s^{-1} for about 100 minutes, the proton density up to 70 cm^{-3} for about 30 minutes, and the IMF up to 70 nT for about 10 minutes. Higher values are possible in case of instrumentation saturation, which is likely for plasma instruments. Based on these statistics, the observational requirements are to measure the IMF up to 150 nT (I-R1), the proton and electron moments for densities up to 80 cm^{-3} and speed up to 1200 km s^{-1} (I-R2, I-R3 and I-R5) to capture all but the most extreme values of the solar wind. As 99.9% of the solar wind reaches 1 au with a

speed below 860 km s^{-1}, it is enough to measure alpha particles for these conditions (I-R7). Alpha particle measurements can be important to identify MEs and other transients. Based on past research, the electron pitch-angle distribution should be measured for energies between about 90 eV and 1 keV (I-R6) to determine the connectivity of magnetic field lines, especially important to investigate CMEs and HCSs. To investigate the acceleration of particles by IP shocks and SIRs, it is necessary to measure ions with energies of 50 keV–5 MeV (I-R8), which are the peak energies for both SIR-accelerated particles and ESPs as well as suprathermal particles of energies of ∼4 keV–15 keV (I-R9) which are likely to be the seeds for these energetic particles. These observation requirements are summarized in Fig. 6 and can be compared to SWFO-L1 or IMAP *in situ* instrument requirements.

MIIST must also measure energetic electrons that are associated with flare acceleration (typically 10 s to 100 of keV, I-R10), which can also be used to trace magnetic field lines. Measuring the solar wind turbulence in the inertial range and the beginning of the dissipation range (∼1 mHz to 2 Hz) is required to determine the importance of solar wind turbulence on the acceleration of these particles. These measurements are also similar to those from SWFO-L1, *Wind*, or from IMAP *in situ* instruments.

For large-scale transients, 2-min temporal resolution is enough as it represents ∼0.2% of the typical duration of a CME magnetic ejecta (20 hours) and ∼0.1% of the typical duration of an SIR (36 hours). To determine shock properties, high-resolution magnetic field data are required (at a cadence of at least 1 measurement per second). ACE and *Wind* measurements and studies have shown how shock properties can be determined accurately by combining high-resolution magnetic field data with lower-resolution plasma data.

For MIIST, the instrument suite is based on those from missions launched over the past two decades or scheduled to launch to measure the inner heliosphere, including STEREO (Kaiser et al. 2008), Solar Orbiter (Müller et al. 2020), PSP (Fox et al. 2016), IMAP (McComas et al. 2018), and SWFO-L1. Figure 6 lists the measurement requirements for such a mission and how they map to the instrument requirements.

These are the minimum requirements for a "threshold" mission that can be submitted as a Small Explorer. A baseline mission may add additional observations and instrument requirements, including (a) a solar wind composition and charge state sensor, (b) a dedicated suprathermal ion instrument building on such instruments on ACE, STEREO, and IMAP, among others, like CODICE on IMAP, (c) a high-energy particle instrument with abundance, to measure protons, helium, and heavier nuclei up to Fe for energies of several 10 s of MeV/nucleon, as well as electrons for energies above 1 MeV, and (d) a radio and plasma wave instrument to measure radio waves as well as local magnetic and electric field. Remote-sensing instruments, such as an X-ray telescope or a coronagraph, may be added but would require a 3-axis stabilized platform, whereas an *in situ* only suite would be simpler with a spin-stabilized or slowly rotating platform (removing the need for deflectors and their associated high-voltage power supplies). We note, however, that the observation requirements as mentioned above are the only ones required to reach the SOs and SWROs and that they can be fully fulfilled with the four instruments listed in Fig. 6 and described below.

3 Implementation: Payload, Requirements on Number of Spacecraft, and Orbit

To fulfill the observational requirements, numerous specific implementations are possible. As detailed above, the measurement requirements are comparable to that of several past missions and can be achieved with high-TRL instruments. The implementation described here

MIIST Science Traceability Matrix

Goal	Science Objectives	Observation Requirements	Instrument	Instrument Parameters	Instrument Requirements
Determine the spatiotemporal variations and the variability of solar wind structures, transients and energetic particles in the near-Earth interplanetary space	**SO1** Characterize the longitudinal and temporal variations in the properties of near-Earth IP structures **SO2** Reveal the near-Earth longitudinal structure and temporal evolution of IP transients	**I-R1** Magnetic field vector ±150 nT with ± 0.25 nT accuracy per axis @ 1s	**SWIM**	Species	Proton and alpha
		I-R2 H^+ N and T w/ 10% accuracy for N ~0.5-80 cm^{-3} @ 2 min **I-R3** H^+ |V| w/ 5% accuracy for |V|~250-1200 km/s @ 2 min		SW Energy Range and Resolution	0.6 - 15 keV/q at ΔE/E = 0.1
				FOV and Angular Resolution	60° (roll) x 60° (elevation) w/ 5° res.
		I-R4 N-S and E-W H^+ flow angles within 5° @ 2 min		Dynamical Range (protons)	0.5 - 80 cm^{-3}
		I-R5 e^- moments for V~250-1,200 km/s with 20% accuracy @ 2 min		Time Resolution	2 min 3D
		I-R6 Suprathermal e^- (80 eV – 1 keV) Pitch Angle Distribution @ 2min	**NEMISIS**	Range, Noise	±150 nT, noise < 0.2 nT/√Hz
		I-R7 He^{2+} moments for V~250-860 km/s @ 2 min w/ 10% accuracy		Accuracy and Resolution	± 0.25 nT per axis; resolution < 50 pT
				Time Resolution	4 vectors/sec (2 Hz Nyquist)
	SO3 Determine how the near-Earth properties of energetic particles accelerated by IP structures and transients depend on the variability in the local conditions and the properties of the drivers	**I-R8** Ions 50 keV - 5 MeV @ 5 min	**EPD**	Energy Range and Resolution	Ions: 50 keV - 5 MeV at ΔE/E = 0.5
		I-R9 Suprathermal Ions 4 keV - 15 keV @ 5 min			Electrons: 50 keV - 200 keV at ΔE/E = 0.5
		I-R10 Electrons 50 keV - 200 keV @ 5 min		Particle Flux Range	10^2 – 3 10^6 $cm^{-2}/s/sr/eV$
		I-R11 Electrons 100 eV - 2 keV @ 5 min		FOV and Angular Resolution	360° (roll) w/ 45° res. x ±75° (elev.) w/ 45° res.
		I-R12 Magnetic field turbulence at 0.01- 2 Hz		Time Resolution	5 min. 3D
		All previous requirements (I-R1 to I-R7)	**EESA**	Energy Range and Resolution	10 eV - 2 keV at ΔE/E = 0.4
Advance the fundamental knowledge necessary to improve space weather forecasting from in situ data	**SO4** Identify how measurements of IP transients sunward of L1 and measurements of IP structures east and west of the Sun-Earth line can best be employed to forecast space weather at Earth	All previous requirements (I-R1 to I-R12)		Energy Flux Range	10^4-10^8 ($eV/cm^2/s/sr/eV$)
				FOV and Angular Resolution	360° (roll) w/ 30°res. x ±90° (elev.) w/ 30° res.
				Dynamical Range	0.5 – 80 cm^{-3}
				Time Resolution	2 min 3D

Fig. 6 MIIST Science Traceability Matrix and Payload Requirements

Table 1 MIIST Nominal Payload, with the payload size given in U = $(10\ \text{cm})^3$

Instrument name	Mass (kg)	Size	Power (W)	Science data rate (bps)	Beacon rate (bps)	TRL	Heritage
Solar Wind Ion Monitor (SWIM)	∼5	∼15-20U	∼4	∼1000	∼20	6-9	PLASTIC SolO/HIS
Magnetometer w/ boom (NEMISIS)	∼2	∼1-2U + boom	∼1	∼1000	∼15	6-9	HERMES GDC
Energetic particle detector (EPD)	∼2.5	∼4-6 U	∼2	∼400	∼20	6-9	MAVEN/SEP THEMIS/SST
Electron ESA (EESA)	∼2	∼3U	∼2	∼1400	∼15	6-9	PSP/SPAN-e MAVEN/SWEA
Total	∼12		∼10	∼3800	∼70		

is one of many possible implementations, one for which the payload is composed of simple, well-understood, and high-heritage instruments that provide all required measurements (as detailed in Fig. 6) of the near-Earth heliosphere to achieve the SOs and SWROs. Table 1 summarizes the instrument size, mass, telemetry rate, and power requirements. To obtain 3-D measurements without deflectors, the particle instruments (SWIM, EESA, and EPD) require a rotating or spin-stabilized platform. The four instruments are based on recently flown instruments with some simplifications. These are all very basic instruments, with similar concepts and principle of operations, as instruments built and flown several decades ago, but with updated electronics. Other implementations than the one presented here can be easily considered, based on other recently flown instruments or proposed designs.

3.1 Instrument Description, Heritage and Data Sufficiency

The proton electrostatic analyzer is referred to as the Solar Wind Ion Monitor (SWIM) and measures (a) solar wind positive ions in the energy/charge (E/q) range ∼0.24 to 30 keV/q and (b) suprathermal positive ions with energies of up to 30 keV/q in the sunward hemisphere. SWIM is a basic electrostatic analyzer (ESA) and detector system, a simplification of similar instruments built by the University of New Hampshire (UNH), primarily STEREO/PLASTIC (Galvin et al. 2008) and SolO/HIS (Livi et al. 2023).

The Electron ESA (EESA) measures solar wind thermal and suprathermal electrons of energy 2 eV–25 keV. It is a direct but incremental evolution of similar instruments built by the Space Sciences Laboratory (SSL) at the University of California at Berkeley (UCB), primarily PSP/SWEAP/SPAN-e (Kasper et al. 2016; Whittlesey et al. 2020), but also MAVEN/SWEA (Mitchell et al. 2016) and THEMIS/ESA (McFadden et al. 2008).

The Energetic Particle Detector (EPD) measures 25 keV–12 MeV ions and 25 keV–300 keV electrons. EPD is a high-heritage instrument built at UCB/SSL based on the MAVEN/SEP instrument (Larson et al. 2015) and the ten SSTs on the five THEMIS SC (Angelopoulos 2008), all of which are still successfully operating as of mid 2024.

The magnetometer is the Noise Eliminating Magnetometer in a Small Integrated System (NEMISIS), a low-power, low-mass, small integrated system composed of one fluxgate magnetometer mounted on a boom and two spacecraft-mounted commercial magneto-inductive magnetometers. NEMISIS provides measurements of the IMF with high sensitivity (<0.2 nT per axis) at 10-vec/s cadence. NEMISIS is identical to the unit that has gone

Table 2 MIIST Orbit and Mission Requirements

Orbit requirements	Mission requirements
O-R1 1° < Max Angular separation < 20°	M-R1 adequate power in all planned orientations
O-R2 Within 1° of ecliptic	M-R2 spin stabilized or rolling
O-R3 Reaches 0.01 – 0.2 AU upstream of L1	M-R3 roll/spin axis knowledge within 0.5°
	M-R4/5 SWIM and EESA FOV unobstructed
O-R4 Reaches > 0.02 AU sunwards along Parker spiral	M-R6 EPD unobstructed FOV – non-Sun pointing
	M-R7 MAG isolated from SC magnetic fields
O-R5 1 SC spends > 20% of time sunward of L1	M-R8 store and downlink 3.8 kbps of data
	M-R9 take data > 90% of time
O-R6 1 SC spends > 20% of time > 1° east of the Sun–Earth line	M-R10 2 years of 4-SC measurements
	M-R11 Provide beacon measurements at > 70 bps

through flight qualification for HERMES (Moldwin et al. 2022) and is built at the NASA Goddard Space Flight Center (GSFC). NEMISIS combines noise cancellation techniques and machine learning algorithms with the measurements from the distributed sensors to provide accurate and precise IMF measurements (Hoffmann and Moldwin 2022; Hoffmann et al. 2023). The fluxgate sensor is placed at the end of a ∼1.5–2 m boom to reduce spacecraft magnetic noise. The boom is built by UCB, based on the THEMIS (Auslander et al. 2008) and ESCAPADE boom design, scaled for MIIST.

During science mode, MIIST plasma and particle instruments (SWIM, EESA, and EPD) provide 60-s and RFGM provides 10-vec/s resolution measurements. The volume of returned data is sufficient to meet the requirements and corresponds to ∼3.8 kbps. In addition, MIIST has a beacon mode which is transmitted when each spacecraft is upstream of L1 and within 0.12 au from Earth to advance the SWROs.

3.2 Number of Spacecraft and Orbit Requirements

Measurements by three spacecraft would enable the investigation of the radius of curvature of shocks and the angular width of energetic particle events, but unless the spacecraft are exactly at the same heliocentric distance, the results would combine temporal (evolution) effects with spatial (variation) effects. As such, four spacecraft are required to achieve closure on all SOs and SWROs. Additionally, a four-spacecraft constellation, similar to what was proposed by St. Cyr et al. (2000) could always have one spacecraft sunward of L1, therefore maximizing the data to advance the SWROs.

Numerous orbits for a variety of launch configurations and launch vehicles allow us to reach the SOs and SWROs. The orbit and mission requirements are summarized in Table 2. Two such classes of orbits are: (i) Sun–Earth distant retrograde orbits (Sun–Earth DROs, see Henon 1969; Stramacchia et al. 2016; Perozzi et al. 2017; St. Cyr et al. 2000), and (ii) heliospheric drifters (Driesman et al. 2008; Allen et al. 2022). DROs have the advantage of providing a stable orbit from which a single spacecraft goes upstream of the L1 point and also to the side of the Sun–Earth line, but they require $\Delta V \sim 300$ m s^{-1} for final orbit insertion, whereas drifters require less propellant and have been already employed for STEREO. These orbits can be reached with small positive characteristic energy, C3 (C3 ~ 5 km^2 s^{-2}), which can be achieved with lunar or Earth flybys starting from a variety of orbits, including cislunar or L1 orbit (see, e.g. Parsay and Folta 2022), or through a direct launch targeting a lunar flyby as demonstrated by STEREO (and *Wind*). As described below, the spacecraft

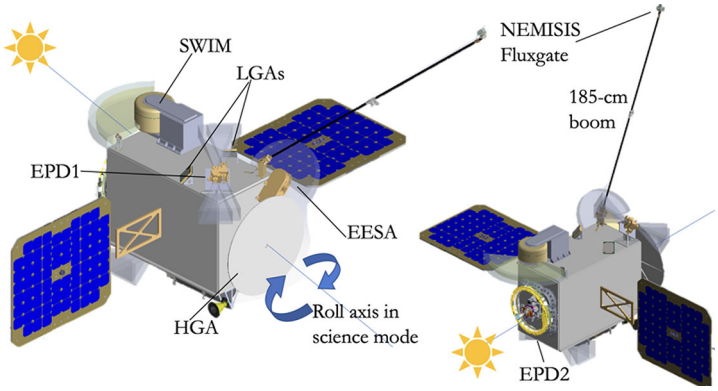

Fig. 7 MIIST spacecraft with payload and field-of-view after deployment. Each MIIST spacecraft rolls slowly during science mode around the Sun-spacecraft line. The magnetometer is on top of 185-cm two-segment boom with additional commercial magnetometers on the spacecraft bus

can easily be built to fit within Evolved Expendable Launch Vehicle (EELV) Secondary Payload Adapter (ESPA) or ESPA Grande class and could be launched one or two at a time as rideshares, or all at once within a 5-m fairing.

4 Implementation: Spacecraft, Orbit, and Communication Strategies

MIIST has been proposed as a 2022 Heliophysics Small Explorers (SMEX) mission concept for a cost cap of 150M in FY2022 $ including cost reserves but excluding launch costs. It builds upon the heritage of numerous missions for its instrumental suites, mission design, and project management, in particular THEMIS, a five-spacecraft MIDEX (Angelopoulos 2008; Harvey et al. 2008) for mission design, PSP, HERMES, and STEREO for the instrumental suite, and ESCAPADE (Lillis et al. 2023) for the spacecraft bus and most subsystems. Without remote-sensing instrumentation, each of the MIIST spacecraft can be spin-stabilized or slowly rolling (taking advantage of 3-axis stabilized commercial spacecraft buses). The maximum distance from Earth would be <0.35 au (based on O-R1), allowing for relatively simple communications and a relatively high data rate. Figure 7 shows the MIIST spacecraft in a deployed configuration with the high gain and low gain antennas (HGA, LGAs) and the instruments as proposed for the 2022 Heliophysics SMEX opportunity.

4.1 Orbit Description and ΔV Requirements

Here, we describe the advantage of using Sun-Earth DROs for MIIST where each spacecraft reaches ∼0.04 au sunward of L1 and ∼6° east of the Sun–Earth line on a DRO. The final orbit of each MIIST spacecraft is a heliocentric orbit with a period of ∼1 year, an average distance from the Sun of ∼1 au, and a small eccentricity that brings it sunward and anti-sunward of Earth's orbit (see left panel of Fig. 8 in IAU Sun Pole coordinates). The orbits are stable, and no active station keeping is needed to maintain the orbit or the spacecraft separation. The spacecraft are phased so that they are 60–90° from one another as seen from Earth. The two-spacecraft separation reaches 0.1 au separation in heliocentric distance and 12° longitudinally for a four-spacecraft constellation.

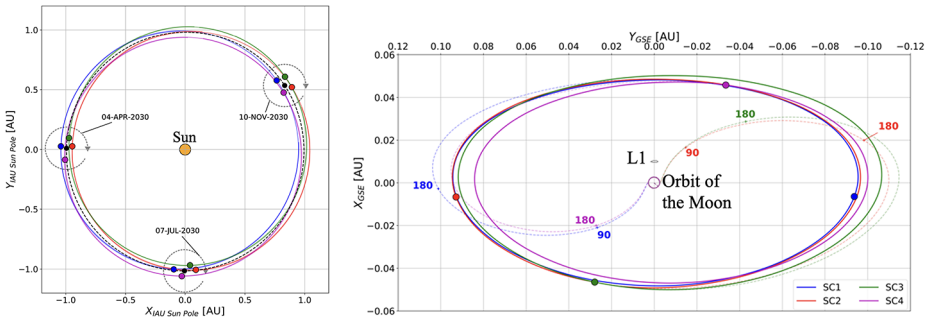

Fig. 8 MIIST Sun–Earth DRO with $d_{min} = 0.048$ AU enables four-spacecraft measurements that meet all science requirements. (a) in IAU Sun pole (Earth's orbit shown with a dashed black line), (b) in GSE coordinates

We assume a launch into a trans-lunar injection (TLI) orbit. Under a very conservative scenario, the spacecraft are assumed to be responsible for the powered lunar flyby and insertion into a Near-Rectilinear Halo Orbit (NRHO) in cislunar space. Phasing between the spacecraft can be obtained by staying longer in the NRHO in cislunar space. The spacecraft exit the NRHO in pairs, with the two spacecraft within each pair exiting two weeks apart, in order to be on dawn and dusk side of Earth. The two pairs leave NRHO two to four months apart. The total ΔV requirement under this scenario is just about 1000 m s^{-1} per spacecraft. If the spacecraft can be dropped in NRHO, the ΔV requirement drops to less than 600 m s^{-1}. A spacecraft with a dry mass of $\sim$100 kg and wet mass of $\sim$160 kg can therefore be considered with chemical propulsion. This enables the launch of four spacecraft on two ESPA Grande ports.

4.2 Telecom Strategy and Beacon Mode

All generated data can be downlinked in 8-hour DSN passes from the HGA to a 34-m station, once every 2–4 weeks, for 1–2 weekly passes. A beacon mode is possible via Near-Earth Network (NEN) antennas for rates of 200 bps–5 kbps for distances up to 0.12 au. This allows the spacecraft to transmit a beacon mode containing real-time solar wind data and housekeeping data when each spacecraft is upstream of L1.

5 Summary and Conclusion

In this paper we present the science justification, science objectives, measurement requirements, and implementation for a small multi-spacecraft mission to investigate large-scale structures and transients by providing *in situ* measurements of the plasma, suprathermal and energetic particles, and interplanetary magnetic field in the near-Earth interplanetary space.

Measurements over the past several decades, primarily from two-spacecraft missions such as Helios and STEREO combined with L1 observatories, but also from fortuitous conjunctions, have provided some strong clues that spatial scales of 0.01–0.25 au ($\sim$0.5–15°) are key to understanding the structure and variations of large-scale transients near Earth. In addition, a space weather research mission is necessary to advance our understanding of how to improve lead time of forecasting space weather drivers, both radially propagating and corotating, from 1 to 4–12 hours. MIIST, as described in this manuscript, can advance

both goals to (a) determine the spatiotemporal variations and the variability of solar wind structures, transients, and energetic particle fluxes in near-Earth IP space, and (b) advance our fundamental knowledge necessary to improve space weather forecasting from *in situ* data. Such a mission would ideally be launched outside of solar minimum, to ensure that a sufficient number of CMEs and IP shocks are measured during the two-year of the prime mission (the number of SIRs remains more constant during the solar cycle). While a launch near solar maximum ensures the maximum number of shocks and CMEs, there tends to be more complex interactions between multiple eruptions, which render the analysis more complex. As such, a launch during the rising phase of the solar cycle might be optimal.

The proposed implementation demonstrates that a mission addressing such compelling science and space weather research questions, similar to that from the Multi-Spacecraft Heliospheric Mission (MHM) from the 2003 Heliophysics Decadal Survey can be performed with a high TRL payload and commercial platform within Small Explorers programmatic (cost, schedule, launch options) constraints. While MHM was one of the top priorities of the Heliophyscics decadal survey more than 20 years ago, there is a dire need for such a mission concept to be implemented in time for the rising and maximum of Solar Cycle 26 (∼2033–2037).

Acknowledgements The team acknowledges the NASA Heliophysics Explorers program whose opportunities resulted in the development of the mission concept presented here. The team thanks additional individuals from UNH, UC Berkeley, and Rocket Lab who worked on additional aspects not presented in this paper.

Funding Scientific studies by N. L., N. A., B. Z., and F. R. that led to the development of the science requirements were funded by 80NSSC21K0463, 80NSSC22K0349, 80NSSC20K0700, 80NSSC23K1057, AGS-1954983, and AGS-2301382. L. J. thanks the support of NASA's STEREO mission and Heliophysics Guest Investigator Grant 80NSSC23K0447. C.M. and E.W. acknowledge funding by the European Union (ERC, HELIO4CAST, 101042188). Views and opinions expressed are however those of the author(s) only and do not necessarily reflect those of the European Union or the European Research Council Executive Agency. Neither the European Union nor the granting authority can be held responsible for them.

Declarations

Competing Interests The authors declare no competing interests.

References

Akhavan-Tafti M, Johnson L, Sood R, Slavin JA, Pulkkinen T, Lepri S, Kilpua E, Fontaine D, Szabo A, Wilson L, Le G, Atilaw TY, Ala-Lahti M, Soni SL, Biesecker D, Jian LK, Lario D (2023) Space weather investigation frontier (SWIFT). Front Astron Space Sci 10:1185603. https://doi.org/10.3389/fspas.2023.1185603

Al-Haddad N, Nieves-Chinchilla T, Möstl C, Hidalgo MA, Marubashi K, Savani MP, Roussev II, Poedts S, Farrugia CJ (2013) Magnetic field configuration models and reconstruction methods for ICMEs: a comparative study. Sol Phys 284:129–149. https://doi.org/10.1007/s11207-013-0244-5

Al-Haddad N, Lugaz N, Poedts S, Farrugia CJ, Nieves-Chinchilla T, Roussev II (2019) Evolution of coronal mass ejection properties in the inner heliosphere: prediction for the Solar Orbiter and Parker Solar Probe. Astrophys J 884(2):179. https://doi.org/10.3847/1538-4357/ab4126

Al-Haddad N, Galvin AB, Lugaz N, Farrugia CJ, Yu W (2022) Investigating the cross sections of coronal mass ejections through the study of nonradial flows with STEREO/PLASTIC. Astrophys J 927(1):68. https://doi.org/10.3847/1538-4357/ac32e1

Ala-Lahti M, Ruohotie J, Good S, Kilpua EKJ, Lugaz N (2020) Spatial coherence of interplanetary coronal mass ejection sheaths at 1 AU. J Geophys Res Space Phys 125(9):2020–028002. https://doi.org/10.1029/2020JA028002

Allen RC, Ho GC, Jian LK, Vines SK, Bale SD, Case AW, Hill ME, Joyce CJ, Kasper JC, Korreck KE, Malaspina DM, McComas DJ, McNutt R, Möstl C, Odstrcil D, Raouafi N, Schwadron NA, Stevens ML (2021) A living catalog of stream interaction regions in the Parker Solar Probe era. Astron Astrophys 650:25. https://doi.org/10.1051/0004-6361/202039833

Allen RC, Smith EJ, Anderson BJ, Borovsky JE, Ho GC, Jian L, Krucker S, Lepri S, Li G, Livi S, Lugaz N, Malaspina DM, Maruca BA, Mostafavi P, Raines JM, Verscharen D, Vievering J, Vines SK, Whittlesey P, Wilson I, Lynn B, Wimmer-Schweingruber RF (2022) Interplanetary mesoscale observatory (InterMeso): a mission to untangle dynamic mesoscale structures throughout the heliosphere. Front Astron Space Sci 9:1002273. https://doi.org/10.3389/fspas.2022.1002273

Angelopoulos V (2008) The THEMIS mission. Space Sci Rev 141(1–4):5–34. https://doi.org/10.1007/s11214-008-9336-1

Arge CN, Pizzo VJ (2000) Improvement in the prediction of solar wind conditions using near-real time solar magnetic field updates. J Geophys Res 105:10465–10480. https://doi.org/10.1029/1999JA900262

Auslander D, Cermenska J, Dalton G, de La Pena M, Dharan CKH, Donokowski W, Duck R, Kim J, Pankow D, Plauche A, Rahmani M, Sulack S, Tan TF, Turin P, Williams T (2008) Instrument boom mechanisms on the THEMIS satellites; magnetometer, radial wire, and axial booms. Space Sci Rev 141(1–4):185–211. https://doi.org/10.1007/s11214-008-9386-4

Bailey RL, Möstl C, Reiss MA, Weiss AJ, Amerstorfer UV, Amerstorfer T, Hinterreiter J, Magnes W, Leonhardt R (2020) Prediction of Dst during solar minimum using in situ measurements at L5. Space Weather 18(5):2019–002424. https://doi.org/10.1029/2019SW002424

Bučík R, Mall U, Korth A, Mason GM (2011) STEREO observations of the energetic ions in tilted corotating interaction regions. J Geophys Res 116(A6):06103. https://doi.org/10.1029/2010JA016311

Burch JL, Moore TE, Torbert RB, Giles BL (2016) Magnetospheric multiscale overview and science objectives. Space Sci Rev 199(1–4):5–21. https://doi.org/10.1007/s11214-015-0164-9

Burlaga L, Sittler E, Mariani F, Schwenn R (1981) Magnetic loop behind an interplanetary shock - Voyager, Helios, and IMP 8 observations. J Geophys Res 86:6673–6684. https://doi.org/10.1029/JA086iA08p06673

Chi Y, Shen C, Scott C, Xu M, Owens M, Wang Y, Lockwood M (2022) Predictive capabilities of corotating interaction regions using STEREO and wind in-situ observations. Space Weather 20(7):2022–003112. https://doi.org/10.1029/2022SW003112

Cohen O, Sokolov IV, Roussev II, Arge CN, Manchester WB, Gombosi TI, Frazin RA, Park H, Butala MD, Kamalabadi F, Velli M (2007) A semiempirical magnetohydrodynamical model of the solar wind. Astrophys J Lett 654:163–166. https://doi.org/10.1086/511154

Cohen CMS, Christian ER, Cummings AC, Davis AJ, Desai MI, Giacalone J, Hill ME, Joyce CJ, Labrador AW, Leske RA, Matthaeus WH, McComas DJ, McNutt JRL, Mewaldt RA, Mitchell DG, Rankin JS, Roelof EC, Schwadron NA, Stone EC, Szalay JR, Wiedenbeck ME, Allen RC, Ho GC, Jian LK, Lario D, Odstrcil D, Bale SD, Badman ST, Pulupa M, MacDowall RJ, Kasper JC, Case AW, Korreck KE, Larson DE, Livi R, Stevens ML, Whittlesey P (2020) Energetic particle increases associated with stream interaction regions. Astrophys J Suppl Ser 246(2):20. https://doi.org/10.3847/1538-4365/ab4c38

Crooker NU, Huang C-L, Lamassa SM, Larson DE, Kahler SW, Spence HE (2004) Heliospheric plasma sheets. J Geophys Res 109(A3):03107. https://doi.org/10.1029/2003JA010170

Davies EE, Forsyth RJ, Winslow RM, Möstl C, Lugaz N (2021) A catalog of interplanetary coronal mass ejections observed by Juno between 1 and 5.4 au. Astrophys J 923(2):136. https://doi.org/10.3847/1538-4357/ac2ccb

Démoulin P, Janvier M, Masías-Meza JJ, Dasso S (2016) Quantitative model for the generic 3D shape of ICMEs at 1 AU. Astron Astrophys 595:19. https://doi.org/10.1051/0004-6361/201628164

Denton MH, Borovsky JE (2008) Superposed epoch analysis of high-speed-stream effects at geosynchronous orbit: hot plasma, cold plasma, and the solar wind. J Geophys Res 113(A7):07216. https://doi.org/10.1029/2007JA012998

Driesman A, Hynes S, Cancro G (2008) The STEREO observatory. Space Sci Rev 136(1–4):17–44. https://doi.org/10.1007/s11214-007-9286-z

Ebert RW, Dayeh MA, Desai MI, Jian LK, Li G, Mason GM (2016) Multi-spacecraft analysis of energetic heavy ion and interplanetary shock properties in energetic storm particle events near 1 au. Astrophys J 831(2):153. https://doi.org/10.3847/0004-637X/831/2/153

Echer E, Gonzalez WD, Tsurutani BT, Gonzalez ALC (2008) Interplanetary conditions causing intense geomagnetic storms (Dst ≤ -100 nT) during solar cycle 23 (1996-2006). J Geophys Res 113:05221. https://doi.org/10.1029/2007JA012744

Echer E, Tsurutani BT, Gonzalez WD (2013) Interplanetary origins of moderate (-100 nT $>$ Dst $>$ -50 nT) geomagnetic storms during solar cycle 23 (1996-2008). J Geophys Res Space Phys 118:385–392. https://doi.org/10.1029/2012JA018086

Escoubet CP, Schmidt R, Goldstein ML (1997) Cluster - science and mission overview. Space Sci Rev 79:11–32. https://doi.org/10.1023/A:1004923124586

Fox NJ, Velli MC, Bale SD, Decker R, Driesman A, Howard RA, Kasper JC, Kinnison J, Kusterer M, Lario D, Lockwood MK, McComas DJ, Raouafi NE, Szabo A (2016) The Solar Probe Plus mission: humanity's first visit to our star. Space Sci Rev 204(1–4):7–48. https://doi.org/10.1007/s11214-015-0211-6

Franz H (2002) A wind trajectory design incorporating multiple transfers between libration points. In: American institute of aeronautics and astronautics. https://doi.org/10.2514/6.2002-4525

Galvin AB, Kistler LM, Popecki MA, Farrugia CJ, Simunac KDC, Ellis L, Möbius E, Lee MA, Boehm M, Carroll J, Crawshaw A, Conti M, Demaine P, Ellis S, Gaidos JA, Googins J, Granoff M, Gustafson A, Heirtzler D, King B, Knauss U, Levasseur J, Longworth S, Singer K, Turco S, Vachon P, Vosbury M, Widholm M, Blush LM, Karrer R, Bochsler P, Daoudi H, Etter A, Fischer J, Jost J, Opitz A, Sigrist M, Wurz P, Klecker B, Ertl M, Seidenschwang E, Wimmer-Schweingruber RF, Koeten M, Thompson B, Steinfeld D (2008) The Plasma and Suprathermal Ion Composition (PLASTIC) investigation on the STEREO observatories. Space Sci Rev 136:437–486. https://doi.org/10.1007/s11214-007-9296-x

Giacalone J, Jokipii JR (2012) The longitudinal transport of energetic ions from impulsive solar flares in interplanetary space. Astrophys J Lett 751:33. https://doi.org/10.1088/2041-8205/751/2/L33

Giacalone J, Jokipii JR, Kóta J (2002) Particle acceleration in solar wind compression regions. Astrophys J 573:845–850. https://doi.org/10.1086/340660

Gómez-Herrero R, Klassen A, Müller-Mellin R, Heber B, Wimmer-Schweingruber R, Böttcher S (2009) Recurrent CIR-accelerated ions observed by STEREO SEPT. J Geophys Res 114(A5):05101. https://doi.org/10.1029/2008JA013755

Harvey P, Taylor E, Sterling R, Cully M (2008) The THEMIS constellation. Space Sci Rev 141(1–4):117–152. https://doi.org/10.1007/s11214-008-9416-2

Henon M (1969) Numerical exploration of the restricted problem, V. Astron Astrophys 1:223–238

Hoffmann AP, Moldwin MB (2022) Separation of spacecraft noise from geomagnetic field observations through density-based cluster analysis and compressive sensing. J Geophys Res Space Phys 127(9):2022–030757. https://doi.org/10.1029/2022JA030757

Hoffmann AP, Moldwin MB, Strabel BP, Ojeda LV (2023) Enabling boomless CubeSat magnetic field measurements with the quad-mag magnetometer and an improved underdetermined blind source separation algorithm. J Geophys Res Space Phys 128(9):2023–031662. https://doi.org/10.1029/2023JA031662

Hofmeister SJ, Asvestari E, Guo J, Heidrich-Meisner V, Heinemann SG, Magdalenic J, Poedts S, Samara E, Temmer M, Vennerstrom S, Veronig A, Vršnak B, Wimmer-Schweingruber R (2022) How the area of solar coronal holes affects the properties of high-speed solar wind streams near Earth: an analytical model. Astron Astrophys 659:190. https://doi.org/10.1051/0004-6361/202141919

Huttunen K, Koskinen H (2004) Importance of post-shock streams and sheath region as drivers of intense magnetospheric storms and high-latitude activity. Ann Geophys 22:1729–1738. https://doi.org/10.5194/angeo-22-1729-2004

Jian L, Russell CT, Luhmann JG, Skoug RM (2006) Properties of stream interactions at one AU during 1995–2004. Sol Phys 239:337–392. https://doi.org/10.1007/s11207-006-0132-3

Jian LK, Russell CT, Luhmann JG, Skoug RM, Steinberg JT (2008a) Stream interactions and interplanetary coronal mass ejections at 0.72 AU. Sol Phys 249(1):85–101. https://doi.org/10.1007/s11207-008-9161-4

Jian LK, Russell CT, Luhmann JG, Skoug RM, Steinberg JT (2008b) Stream interactions and interplanetary coronal mass ejections at 5.3 AU near the solar ecliptic plane. Sol Phys 250(2):375–402. https://doi.org/10.1007/s11207-008-9204-x

Jian LK, Russell CT, Luhmann JG, Galvin AB, MacNeice PJ (2009) Multi-spacecraft observations: stream interactions and associated structures. Sol Phys 259(1–2):345. https://doi.org/10.1007/s11207-009-9445-3

Jian LK, Russell CT, Luhmann JG, Galvin AB (2018) STEREO observations of interplanetary coronal mass ejections in 2007–2016. Astrophys J 855:114. https://doi.org/10.3847/1538-4357/aab189

Jian LK, Luhmann JG, Russell CT, Galvin AB (2019) Solar Terrestrial Relations Observatory (STEREO) observations of stream interaction regions in 2007 - 2016: relationship with heliospheric current sheets,

solar cycle variations, and dual observations. Sol Phys 294(3):31. https://doi.org/10.1007/s11207-019-1416-8

Kaiser ML, Kucera TA, Davila JM, St. Cyr OC, Guhathakurta M, Christian E (2008) The STEREO mission: an introduction. Space Sci Rev 136:5–16. https://doi.org/10.1007/s11214-007-9277-0

Kasper JC, Abiad R, Austin G, Balat-Pichelin M, Bale SD, Belcher JW, Berg P, Bergner H, Berthomier M, Bookbinder J, Brodu E, Caldwell D, Case AW, Chandran BDG, Cheimets P, Cirtain JW, Cranmer SR, Curtis DW, Daigneau P, Dalton G, Dasgupta B, DeTomaso D, Diaz-Aguado M, Djordjevic B, Donaskowski B, Effinger M, Florinski V, Fox N, Freeman M, Gallagher D, Gary SP, Gauron T, Gates R, Goldstein M, Golub L, Gordon DA, Gurnee R, Guth G, Halekas J, Hatch K, Heerikuisen J, Ho G, Hu Q, Johnson G, Jordan SP, Korreck KE, Larson D, Lazarus AJ, Li G, Livi R, Ludlam M, Maksimovic M, McFadden JP, Marchant W, Maruca BA, McComas DJ, Messina L, Mercer T, Park S, Peddie AM, Pogorelov N, Reinhart MJ, Richardson JD, Robinson M, Rosen I, Skoug RM, Slagle A, Steinberg JT, Stevens ML, Szabo A, Taylor ER, Tiu C, Turin P, Velli M, Webb G, Whittlesey P, Wright K, Wu ST, Zank G (2016) Solar Wind Electrons Alphas and Protons (SWEAP) investigation: design of the solar wind and coronal plasma instrument suite for Solar Probe Plus. Space Sci Rev 204(1–4):131–186. https://doi.org/10.1007/s11214-015-0206-3

Kay C, Nieves-Chinchilla T, Hofmeister SJ, Palmerio E (2023) An efficient, time-dependent high speed stream model and application to solar wind forecasts. Space Weather 21(5):2023–003443. https://doi.org/10.1029/2023SW003443

Kay C, Palmerio E, Riley P, Mays ML, Nieves-Chinchilla T, Romano M, Collado-Vega YM, Wiegand C, Chulaki A (2024) Updating measures of CME arrival time errors. Space Weather 22(7):2024–003951. https://doi.org/10.1029/2024SW003951

Kilpua EKJ, Lee CO, Luhmann JG, Li Y (2011) Interplanetary coronal mass ejections in the near-Earth solar wind during the minimum periods following solar cycles 22 and 23. Ann Geophys 29:1455–1467. https://doi.org/10.5194/angeo-29-1455-2011

Kilpua E, Koskinen HEJ, Pulkkinen TI (2017) Coronal mass ejections and their sheath regions in interplanetary space. Living Rev Sol Phys 14:5. https://doi.org/10.1007/s41116-017-0009-6

Klein KG, Spence H, Alexandrova O, Argall M, Arzamasskiy L, Bookbinder J, Broeren T, Caprioli D, Case A, Chandran B, Chen L-J, Dors I, Eastwood J, Forsyth C, Galvin A, Genot V, Halekas J, Hesse M, Hine B, Horbury T, Jian L, Kasper J, Kretzschmar M, Kunz M, Lavraud B, Le Contel O, Mallet A, Maruca B, Matthaeus W, Niehof J, O'Brien H, Owen C, Retinò A, Reynolds C, Roberts O, Schekochihin A, Skoug R, Smith C, Smith S, Steinberg J, Stevens M, Szabo A, TenBarge J, Torbert R, Vasquez B, Verscharen D, Whittlesey P, Wickizer B, Zank G, Zweibel E (2023) HelioSwarm: a multipoint, multiscale mission to characterize turbulence. Space Sci Rev 219(8):74. https://doi.org/10.1007/s11214-023-01019-0

Kouloumvakos A, Kwon RY, Rodríguez-García L, Lario D, Dresing N, Kilpua EKJ, Vainio R, Török T, Plotnikov I, Rouillard AP, Downs C, Linker JA, Malandraki OE, Pinto RF, Riley P, Allen RC (2022) The first widespread solar energetic particle event of solar cycle 25 on 2020 November 29. Shock wave properties and the wide distribution of solar energetic particles. Astron Astrophys 660:84. https://doi.org/10.1051/0004-6361/202142515

Koval A, Szabo A (2008) Modified "Rankine-Hugoniot" shock fitting technique: simultaneous solution for shock normal and speed. J Geophys Res 113(A10):10110. https://doi.org/10.1029/2008JA013337

Koval A, Szabo A (2010) Multispacecraft observations of interplanetary shock shapes on the scales of the Earth's magnetosphere. J Geophys Res 115(A12):12105. https://doi.org/10.1029/2010JA015373

Kubicka M, Möstl C, Amerstorfer T, Boakes PD, Feng L, Eastwood JP, Törmänen O (2016) Prediction of geomagnetic storm strength from inner heliospheric in situ observations. Astrophys J 833(2):255. https://doi.org/10.3847/1538-4357/833/2/255

Laker R, Horbury TS, O'Brien H, Fauchon-Jones EJ, Angelini V, Fargette N, Amerstorfer T, Bauer M, Möstl C, Davies EE, Davies JA, Harrison R, Barnes D, Dumbović M (2024) Using Solar Orbiter as an upstream solar wind monitor for real time space weather predictions. Space Weather 22(2):2023–003628. https://doi.org/10.1029/2023SW003628

Lario D, Ho GC, Decker RB, Roelof EC, Desai MI, Smith CW (2003) ACE observations of energetic particles associated with transient interplanetary shocks. In: Velli M, Bruno R, Malara F, Bucci B (eds) Solar wind ten. American institute of physics conference series, vol 679, pp 640–643. https://doi.org/10.1063/1.1618676

Larson DE, Lillis RJ, Lee CO, Dunn PA, Hatch K, Robinson M, Glaser D, Chen J, Curtis D, Tiu C, Lin RP, Luhmann JG, Jakosky BM (2015) The MAVEN solar energetic particle investigation. Space Sci Rev 195(1–4):153–172. https://doi.org/10.1007/s11214-015-0218-z

Lee MA, Mewaldt RA, Giacalone J (2012) Shock acceleration of ions in the heliosphere. Space Sci Rev 173(1–4):247–281. https://doi.org/10.1007/s11214-012-9932-y

Lepping RP, Jones JA, Burlaga LF (1990) Magnetic field structure of interplanetary magnetic clouds at 1 AU. J Geophys Res 95(A8):11957–11965. https://doi.org/10.1029/JA095iA08p11957

Lillis RJ, Curry SM, Curtis DW, Taylor ER, Courtade SE, Ma YJ, Parker J, Hara T, Luhmann JG, Barjatya A, Espley J, Gruesbeck J, Sarantos M, Larson D, Livi R, Whittlesey P, Modolo R, Harada Y, Fowler CM, Xu SS, Brain DA, Thiemann EMB, Mosleh E, Mandy C (2023) ESCAPADE update: a twin spacecraft SIMPLEX mission to unveil Mars' unique hybrid magnetosphere. In: LPI contributions, vol 2806, p 1108

Lindsay GM, Russell CT, Luhmann JG (1999) Predictability of Dst index based upon solar wind conditions monitored inside 1 AU. J Geophys Res 104(A5):10335–10344. https://doi.org/10.1029/1999JA900010

Liu Y, Manchester WB, Richardson JD, Luhmann JG, Lin RP, Bale SD (2008) Deflection flows ahead of ICMEs as an indicator of curvature and geoeffectiveness. J Geophys Res 113(A12):A00B03. https://doi.org/10.1029/2007JA012996

Liu YD, Luhmann JG, Kajdič P, Kilpua EKJ, Lugaz N, Nitta NV, Möstl C, Lavraud B, Bale SD, Farrugia CJ, Galvin AB (2014) Observations of an extreme storm in interplanetary space caused by successive coronal mass ejections. Nat Commun 5:3481. https://doi.org/10.1038/ncomms4481

Livi S, Lepri ST, Raines JM, Dewey RM, Galvin AB, Louarn P, Collier MR, Allegrini F, Alterman BL, Bert CM, Bruno R, Chornay DJ, D'Amicis R, Eddy TJ, Ellis L, Fauchon-Jones E, Fedorov A, Gershkovich I, Holmes J, Horbury TS, Kistler LM, Kucharek H, Lugaz N, Nieves-Chinchilla T, O'Brien H, Ogasawara K, Owen CJ, Phillips M, Ploof K, Rivera YJ, Spitzer SA, Stubbs TJ, Wurz P (2023) First results from the Solar Orbiter heavy ion sensor. Astron Astrophys 676:36. https://doi.org/10.1051/0004-6361/202346304

Lugaz N, Farrugia CJ, Winslow RM, Al-Haddad N, Kilpua EKJ, Riley P (2016) Factors affecting the geoeffectiveness of shocks and sheaths at 1 AU. J Geophys Res Space Phys 121(A10):10. https://doi.org/10.1002/2016JA023100

Lugaz N, Farrugia CJ, Winslow RM, Al-Haddad N, Galvin AB, Nieves-Chinchilla T, Lee CO, Janvier M (2018) On the spatial coherence of magnetic ejecta: measurements of coronal mass ejections by multiple spacecraft longitudinally separated by 0.01 au. Astrophys J Lett 864:7. https://doi.org/10.3847/2041-8213/aad9f4

Lugaz N, Salman TM, Zhuang B, Al-Haddad N, Scolini C, Farrugia CJ, Yu W, Winslow RM, Möstl C, Davies EE, Galvin AB (2022) A coronal mass ejection and magnetic ejecta observed in situ by STEREO-A and wind at 55° angular separation. Astrophys J 929(2):149. https://doi.org/10.3847/1538-4357/ac602f

Lugaz N, Zhuang B, Scolini C, Al-Haddad N, Farrugia CJ, Winslow RM, Regnault F, Möstl C, Davies EE, Galvin AB (2024) The width of magnetic ejecta measured near 1 au: lessons from STEREO-a measurements in 2021–2022. Astrophys J 962(2):193. https://doi.org/10.3847/1538-4357/ad17b9

Lynch BJ, Li Y, Thernisien AFR, Robbrecht E, Fisher GH, Luhmann JG, Vourlidas A (2010) Sun to 1 AU propagation and evolution of a slow streamer-blowout coronal mass ejection. J Geophys Res 115(A14):7106. https://doi.org/10.1029/2009JA015099

Manchester W, Kilpua EKJ, Liu YD, Lugaz N, Riley P, Török T, Vršnak B (2017) The physical processes of CME/ICME evolution. Space Sci Rev 212:1159–1219. https://doi.org/10.1007/s11214-017-0394-0

Mauk BH, Fox NJ, Kanekal SG, Kessel RL, Sibeck DG, Ukhorskiy A (2013) Science objectives and rationale for the radiation belt storm probes mission. Space Sci Rev 179(1–4):3–27. https://doi.org/10.1007/s11214-012-9908-y

McComas DJ, Christian ER, Schwadron NA, Fox N, Westlake J, Allegrini F, Baker DN, Biesecker D, Bzowski M, Clark G, Cohen CMS, Cohen I, Dayeh MA, Decker R, de Nolfo GA, Desai MI, Ebert RW, Elliott HA, Fahr H, Frisch PC, Funsten HO, Fuselier SA, Galli A, Galvin AB, Giacalone J, Gkioulidou M, Guo F, Horanyi M, Isenberg P, Janzen P, Kistler LM, Korreck K, Kubiak MA, Kucharek H, Larsen BA, Leske RA, Lugaz N, Luhmann J, Matthaeus W, Mitchell D, Moebius E, Ogasawara K, Reisenfeld DB, Richardson JD, Russell CT, Sokół JM, Spence HE, Skoug R, Sternovsky Z, Swaczyna P, Szalay JR, Tokumaru M, Wiedenbeck ME, Wurz P, Zank GP, Zirnstein EJ (2018) Interstellar Mapping and Acceleration Probe (IMAP): a new NASA mission. Space Sci Rev 214(8):116. https://doi.org/10.1007/s11214-018-0550-1

McFadden JP, Carlson CW, Larson D, Ludlam M, Abiad R, Elliott B, Turin P, Marckwordt M, Angelopoulos V (2008) The THEMIS ESA plasma instrument and in-flight calibration. Space Sci Rev 141(1–4):277–302. https://doi.org/10.1007/s11214-008-9440-2

Mitchell DL, Mazelle C, Sauvaud J-A, Thocaven J-J, Rouzaud J, Fedorov A, Rouger P, Toublanc D, Taylor E, Gordon D, Robinson M, Heavner S, Turin P, Diaz-Aguado M, Curtis DW, Lin RP, Jakosky BM (2016) The MAVEN solar wind electron analyzer. Space Sci Rev 200(1–4):495–528. https://doi.org/10.1007/s11214-015-0232-1

Miyoshi Y, Kataoka R, Kasahara Y, Kumamoto A, Nagai T, Thomsen MF (2013) High-speed solar wind with southward interplanetary magnetic field causes relativistic electron flux enhancement of the outer radiation belt via enhanced condition of whistler waves. Geophys Res Lett 40(17):4520–4525. https://doi.org/10.1002/grl.50916

Moldwin MB, Ford S, Lepping R, Slavin J, Szabo A (2000) Small-scale magnetic flux ropes in the solar wind. Geophys Res Lett 27(1):57–60. https://doi.org/10.1029/1999GL010724

Moldwin MB, Wilcox E, Zesta E, Bonalsky TM (2022) Single-event effect testing of the PNI RM3100 magnetometer for space applications. Geosci Instrum Method Data Syst 11(1):219–222. https://doi.org/10.5194/gi-11-219-2022

Möstl C, Farrugia CJ, Biernat HK, Leitner M, Kilpua EKJ, Galvin AB, Luhmann JG (2009) Optimized grad - Shafranov reconstruction of a magnetic cloud using STEREO- wind observations. Sol Phys 256:427–441. https://doi.org/10.1007/s11207-009-9360-7

Möstl C, Amerstorfer T, Palmerio E, Isavnin A, Farrugia CJ, Lowder C, Winslow RM, Donnerer JM, Kilpua EKJ, Boakes PD (2018) Forward modeling of coronal mass ejection flux ropes in the inner heliosphere with 3DCORE. Space Weather 16:216–229. https://doi.org/10.1002/2017SW001735

Müller D, St. Cyr OC, Zouganelis I, Gilbert HR, Marsden R, Nieves-Chinchilla T, Antonucci E, Auchère F, Berghmans D, Horbury TS, Howard RA, Krucker S, Maksimovic M, Owen CJ, Rochus P, Rodriguez-Pacheco J, Romoli M, Solanki SK, Bruno R, Carlsson M, Fludra A, Harra L, Hassler DM, Livi S, Louarn P, Peter H, Schühle U, Teriaca L, del Toro Iniesta JC, Wimmer-Schweingruber RF, Marsch E, Velli M, De Groof A, Walsh A, Williams D (2020) The Solar Orbiter mission. Science overview. Astron Astrophys 642:1. https://doi.org/10.1051/0004-6361/202038467

Mulligan T, Reinard AA, Lynch BJ (2013) Advancing in situ modeling of ICMEs: new techniques for new observations. J Geophys Res Space Phys 118(4):1410–1427. https://doi.org/10.1002/jgra.50101

National Research Council (2003) The Sun to the Earth – and beyond: a decadal research strategy in solar and space physics. The National Academies Press, Washington. https://doi.org/10.17226/10477

Neugebauer M, Giacalone J (2005) Multispacecraft observations of interplanetary shocks: nonplanarity and energetic particles. J Geophys Res 110(A12):12106. https://doi.org/10.1029/2005JA011380

Neugebauer M, Giacalone J, Chollet E, Lario D (2006) Variability of low-energy ion flux profiles on interplanetary shock fronts. J Geophys Res 111(A12):12107. https://doi.org/10.1029/2006JA011832

Nieves-Chinchilla T, Vourlidas A, Raymond JC, Linton MG, Al-Haddad N, Savani NP, Szabo A, Hidalgo MA (2018) Understanding the internal magnetic field configurations of ICMEs using more than 20 years of wind observations. Sol Phys 293:25. https://doi.org/10.1007/s11207-018-1247-z

Oliveira DM, Raeder J (2015) Impact angle control of interplanetary shock geoeffectiveness: a statistical study. J Geophys Res Space Phys 120:4313–4323. https://doi.org/10.1002/2015JA021147

Oliveira DM, Arel D, Raeder J, Zesta E, Ngwira CM, Carter BA, Yizengaw E, Halford AJ, Tsurutani BT, Gjerloev JW (2018) Geomagnetically induced currents caused by interplanetary shocks with different impact angles and speeds. Space Weather 16(6):636–647. https://doi.org/10.1029/2018SW001880

Owens MJ, Crooker NU (2006) Coronal mass ejections and magnetic flux buildup in the heliosphere. J Geophys Res 111(A10):10104. https://doi.org/10.1029/2006JA011641

Palmerio E, Carcaboso F, Khoo LY, Salman TM, Sánchez-Cano B, Lynch BJ, Rivera YJ, Pal S, Nieves-Chinchilla T, Weiss AJ, Lario D, Mieth JZD, Heyner D, Stevens ML, Romeo OM, Zhukov AN, Rodriguez L, Lee CO, Cohen CMS, Rodríguez-García L, Whittlesey PL, Dresing N, Oleynik P, Jebaraj IC, Fischer D, Schmid D, Richter I, Auster H-U, Fraschetti F, Mierla M (2024) On the mesoscale structure of coronal mass ejections at Mercury's orbit: BepiColombo and Parker Solar Probe observations. Astrophys J 963(2):108. https://doi.org/10.3847/1538-4357/ad1ab4

Palomba M, Luntama J-P (2022) Vigil: ESA space weather mission in L5. In: 44th COSPAR scientific assembly. Held 16-24 July 2022, p 3544

Parsay K, Folta DC (2022) Transfer to distant retrograde orbits via rideshare to sun-Earth L1 point. J Guid Control Dyn 45(1):179–184. https://doi.org/10.2514/1.G005991

Perozzi E, Ceccaroni M, Valsecchi GB, Rossi A (2017) Distant retrograde orbits and the asteroid hazard. Eur Phys J Plus 132(8):367. https://doi.org/10.1140/epjp/i2017-11644-0

Pfaff JRF (2016) An overview of the scientific and space weather motivation for the "notional" geospace dynamics constellation mission. In: AGU Fall Meeting abstracts, pp 23–01

Raouafi NE, Matteini L, Squire J, Badman ST, Velli M, Klein KG, Chen CHK, Matthaeus WH, Szabo A, Linton M, Allen RC, Szalay JR, Bruno R, Decker RB, Akhavan-Tafti M, Agapitov OV, Bale SD, Bandyopadhyay R, Battams K, Berčič L, Bourouaine S, Bowen TA, Cattell C, Chandran BDG, Chhiber R, Cohen CMS, D'Amicis R, Giacalone J, Hess P, Howard RA, Horbury TS, Jagarlamudi VK, Joyce CJ, Kasper JC, Kinnison J, Laker R, Liewer P, Malaspina DM, Mann I, McComas DJ, Niembro-Hernandez T, Nieves-Chinchilla T, Panasenco O, Pokorný P, Pusack A, Pulupa M, Perez JC, Riley P, Rouillard AP, Shi C, Stenborg G, Tenerani A, Verniero JL, Viall N, Vourlidas A, Wood BE, Woodham LD, Woolley T (2023) Parker Solar Probe: four years of discoveries at solar cycle minimum. Space Sci Rev 219(1):8. https://doi.org/10.1007/s11214-023-00952-4

Reames DV (2013) The two sources of solar energetic particles. Space Sci Rev 175(1–4):53–92. https://doi.org/10.1007/s11214-013-9958-9

Regnault F, Al-Haddad N, Lugaz N, Farrugia CJ, Yu W, Davies EE, Galvin AB, Zhuang B (2023) Investigating the magnetic structure of interplanetary coronal mass ejections using simultaneous multispacecraft in situ measurements. Astrophys J 957(1):49. https://doi.org/10.3847/1538-4357/acef16

Regnault F, Al-Haddad N, Lugaz N, Farrugia CJ, Yu W, Zhuang B, Davies EE (2024a) Discrepancies in the properties of a coronal mass ejection on scales of 0.03 au as revealed by simultaneous measurements at Solar Orbiter and wind: the 2021 November 3–5 event. Astrophys J 962(2):190. https://doi.org/10.3847/1538-4357/ad1883

Regnault F, Al-Haddad N, Lugaz N, Farrugia CJ, Zhuang B, Yu W, Strugarek A (2024b) Exploring the impact of the aging effect on inferred properties of solar coronal mass ejections. Astrophys J Lett 966(1):17. https://doi.org/10.3847/2041-8213/ad3806

Richardson IG (2018) Solar wind stream interaction regions throughout the heliosphere. Living Rev Sol Phys 15(1):1. https://doi.org/10.1007/s41116-017-0011-z

Riley P, Mays ML, Andries J, Amerstorfer T, Biesecker D, Delouille V, Dumbović M, Feng X, Henley E, Linker JA, Möstl C, Nuñez M, Pizzo V, Temmer M, Tobiska WK, Verbeke C, West MJ, Zhao X (2018) Forecasting the arrival time of coronal mass ejections: analysis of the CCMC CME scoreboard. Space Weather 16(9):1245–1260. https://doi.org/10.1029/2018SW001962

Smith EJ (2001) The heliospheric current sheet. J Geophys Res 106(A8):15819–15832. https://doi.org/10.1029/2000JA000120

Smith CW, McCracken KG, Schwadron NA, Goelzer ML (2014) The heliospheric magnetic flux, solar wind proton flux, and cosmic ray intensity during the coming solar minimum. Space Weather 12(7):499–507. https://doi.org/10.1002/2014SW001067

Souza VM, Lopez RE, Jauer PR, Sibeck DG, Pham K, Da Silva LA, Marchezi JP, Alves LR, Koga D, Medeiros C, Rockenbach M, Gonzalez WD (2017) Acceleration of radiation belt electrons and the role of the average interplanetary magnetic field B_z component in high-speed streams. J Geophys Res Space Phys 122(10):10084–10101. https://doi.org/10.1002/2017JA024187

St. Cyr OC, Plunkett SP, Michels DJ, Paswaters SE, Koomen MJ, Simnett GM, Thompson BJ, Gurman JB, Schwenn R, Webb DF, Hildner E, Lamy PL (2000) Properties of coronal mass ejections: SOHO LASCO observations from January 1996 to June 1998. J Geophys Res 105:18169–18186. https://doi.org/10.1029/1999JA000381

Stevens ML, Korreck K, Case T, Kasper J, Prchlik J, Koval A, Szabo A, Biesecker D (2018) L1 constellation evaluation of the Rankine-Hugoniot shock estimation method. In: Solar Heliospheric and INterplanetary Environment (SHINE 2018), p 226

Stramacchia M, Colombo C, Bernelli-Zazzera F (2016) Distant retrograde orbits for space-based near Earth objects detection. Adv Space Res 58(6):967–988. https://doi.org/10.1016/j.asr.2016.05.053

Szabo A, Ho G, Jian L, Lario D, Nieves-Chinchilla T (2023) ICME structure and evolution in the inner heliosphere. Bull Am Astron Soc 55:384. https://doi.org/10.3847/25c2cfeb.7fb78e78

Thomas SR, Fazakerley A, Wicks RT, Green L (2018) Evaluating the skill of forecasts of the near-Earth solar wind using a space weather monitor at L5. Space Weather 16(7):814–828. https://doi.org/10.1029/2018SW001821

Tsurutani BT, Gonzalez WD, Gonzalez ALC, Guarnieri FL, Gopalswamy N, Grande M, Kamide Y, Kasahara Y, Lu G, Mann I, McPherron R, Soraas F, Vasyliunas V (2006) Corotating solar wind streams and recurrent geomagnetic activity: a review. J Geophys Res 111(A7):07. https://doi.org/10.1029/2005JA011273

van der Holst B, Sokolov IV, Meng X, Jin M, Manchester WB IV, Tóth G, Gombosi TI (2014) Alfvén Wave Solar Model (AWSoM): coronal heating. Astrophys J 782:81. https://doi.org/10.1088/0004-637X/782/2/81

Vinas AF, Scudder JD (1986) Fast and optimal solution to the "Rankine-Hugoniot problem". J Geophys Res 91(A1):39–58. https://doi.org/10.1029/JA091iA01p00039

Vourlidas A, Turner D, Biesecker D, Coster A, Engell A, Ho G, Immel T, Keys C, Lanzerotti L, Lu G, Lugaz N, Luhmann J, Leila Mays M, O'Brien P, Semones E, Spence H, Upton L, White S, Spann J (2023) The NASA space weather science and observation gap analysis. Adv Space Res. https://doi.org/10.1016/j.asr.2023.06.046. In press

West J (2005) The geostorm warning mission: Enhanced opportunities based on new technology. 14th AAS/AIAA Space Flight Mechanics Conference 102

Whittlesey PL, Larson DE, Kasper JC, Halekas J, Abatcha M, Abiad R, Berthomier M, Case AW, Chen J, Curtis DW, Dalton G, Klein KG, Korreck KE, Livi R, Ludlam M, Marckwordt M, Rahmati A, Robinson M, Slagle A, Stevens ML, Tiu C, Verniero JL (2020) The Solar Probe ANalyzers—electrons on the Parker Solar Probe. Astrophys J Suppl Ser 246(2):74. https://doi.org/10.3847/1538-4365/ab7370

Wilson I, Lynn B, Brosius AL, Gopalswamy N, Nieves-Chinchilla T, Szabo A, Hurley K, Phan T, Kasper JC, Lugaz N, Richardson IG, Chen CHK, Verscharen D, Wicks RT, TenBarge JM (2021) A quarter century of wind spacecraft discoveries. Rev Geophys 59(2):2020–000714. https://doi.org/10.1029/2020RG000714

Winslow RM, Lugaz N, Schwadron NA, Farrugia CJ, Yu W, Raines JM, Mays ML, Galvin AB, Zurbuchen TH (2016) Longitudinal conjunction between MESSENGER and STEREO a: development of ICME complexity through stream interactions. J Geophys Res Space Phys 121:6092–6106. https://doi.org/10.1002/2015JA022307

Winslow RM, Lugaz N, Scolini C, Galvin AB (2021) First simultaneous in situ measurements of a coronal mass ejection by Parker Solar Probe and STEREO-A. Astrophys J 916(2):94. https://doi.org/10.3847/1538-4357/ac0821

Winslow RM, Scolini C, Lugaz N, Schwadron NA, Galvin AB (2023) On the contribution of coronal mass ejections to the heliospheric magnetic flux budget on different time scales. Astrophys J 958(1):41. https://doi.org/10.3847/1538-4357/ad02f2

Winterhalter D, Smith EJ, Burton ME, Murphy N, McComas DJ (1994) The heliospheric plasma sheet. J Geophys Res 99(A4):6667–6680. https://doi.org/10.1029/93JA03481

Yu W, Farrugia CJ, Lugaz N, Galvin AB, Kilpua EKJ, Kucharek H, Möstl C, Leitner M, Torbert RB, C. Simunac KD, Luhmann JG, Szabo A, Wilson LB, Ogilvie KW, Sauvaud J-A (2014) A statistical analysis of properties of small transients in the solar wind 2007-2009: STEREO and Wind observations. J Geophys Res Space Phys 119:689–708. https://doi.org/10.1002/2013JA019115

Zhang J, Richardson IG, Webb DF, Gopalswamy N, Huttunen E, Kasper JC, Nitta NV, Poomvises W, Thompson BJ, Wu C-C, Yashiro S, Zhukov AN (2007) Solar and interplanetary sources of major geomagnetic storms (Dst < -100 nT) during 1996-2005. J Geophys Res 112(A11):A10102. https://doi.org/10.1029/2007JA012321

Authors and Affiliations

Noé Lugaz[1] · Christina O. Lee[2] · Nada Al-Haddad[1] · Robert J. Lillis[2] · Lan K. Jian[3] · David W. Curtis[2] · Antoinette B. Galvin[1] · Phyllis L. Whittlesey[2] · Ali Rahmati[2] · Eftyhia Zesta[3] · Mark Moldwin[4] · Errol J. Summerlin[3] · Davin E. Larson[2] · Sasha Courtade[2] · Richard French[5] · Richard Hunter[5] · Federico Covitti[5] · Daniel Cosgrove[2] · J.D. Prall[5] · Robert C. Allen[6] · Bin Zhuang[1] · Réka M. Winslow[1] · Camilla Scolini[1,7] · Benjamin J. Lynch[2,8] · Rachael J. Filwett[9] · Erika Palmerio[10] · Charles J. Farrugia[1] · Charles W. Smith[1] · Christian Möstl[11] · Eva Weiler[11] · Miho Janvier[12] · Florian Regnault[1] · Roberto Livi[2] · Teresa Nieves-Chinchilla[3]

✉ N. Lugaz
noe.lugaz@unh.edu

1 Institute for the Study of Earth, Oceans, and Space, University of New Hampshire, Durham, NH 03824, USA

2 Space Sciences Laboratory, University of California, Berkeley, CA 94720, USA

3 Heliophysics Science Division, NASA Goddard Space Flight Center, Greenbelt, MD 20771, USA

4 Department of Climate and Space Sciences and Engineering, University of Michigan, Ann Arbor, MI 48109, USA

5 Rocket Lab USA, Inc., Long Beach, CA 90808, USA

6 Southwest Research Institute, San Antonio, TX 78238, USA

7 Solar–Terrestrial Centre of Excellence, Royal Observatory of Belgium, B-1180 Brussels, Belgium

8 Department of Earth, Planetary, and Space Sciences, University of California, Los Angeles, CA 90095, USA

[9] Department of Physics, Montana State University, Bozeman, MT 59717, USA

[10] Predictive Science Inc., San Diego, CA 92121, USA

[11] Austrian Space Weather Office, GeoSphere Austria, A-8020 Graz, Austria

[12] Université Paris-Saclay, CNRS, Institut d'Astrophysique Spatiale, F-91405 Orsay, France